

Supporting information for

**{Amino-alkoxy-bis(phenolate)}-Scandium versus Yttrium Complexes for the Ring-Opening Polymerization of Lactide and  $\beta$ -Butyrolactone.**

Yulia Chapurina,<sup>a</sup> Joice Klitzke,<sup>a,b</sup> Osvaldo de L. Casagrande Jr,<sup>b</sup> Mouhamad Awada,<sup>a</sup> Vincent Dorcet,<sup>c</sup> Evgeni Kirillov<sup>a</sup> and Jean-François Carpentier<sup>a</sup>

<sup>a</sup> Institut des Sciences Chimiques de Rennes, Organometallics: Materials and Catalysis laboratories, UMR 6226 CNRS-Université de Rennes 1, F-35042 Rennes Cedex, France

<sup>b</sup> Instituto de Química, Laboratório de Catálise Molecular, Universidade Federal do Rio Grande do Sul, Av. Bento Gonçalves, 9500, Porto Alegre, RS 90501-970, Brazil

<sup>c</sup> Institut des Sciences Chimiques de Rennes, Centre de diffraction X, UMR 6226 CNRS-Université de Rennes 1, F-35042 Rennes Cedex, France

## Contents

**Figure S1.** Crystal structures of pro-ligands **L1**, **L2** and **L3**.

**Figure S2.** Solid-state molecular structure of  $\text{Sc}\{\text{ONNO}^{\text{Cum},\text{Me}}\}(\text{N}(\text{SiHMe}_2)_2)$  (**Sc-1**).

**Figure S3.** Solid-state molecular structure of  $\text{Sc}\{\text{ONOO}^{\text{Cum},\text{Cum}}\}(\text{N}(\text{SiHMe}_2)_2)$  (**Sc-3**).

**Figure S4.** Solid-state molecular structure of  $\text{Sc}\{\text{ONOO}^{\text{CumCl},\text{Me}}\}(\text{N}(\text{SiHMe}_2)_2)$  (**Sc-4**).

**Figure S5.** Solid-state molecular structure of  $\text{Y}\{\text{ONOO}^{\text{Cum},\text{Me}}\}(\text{N}(\text{SiHMe}_2)_2)\text{THF}$  (**Y-2**).

**Table S1.** Selected bond distances ( $\text{\AA}$ ) and angles (deg) for pro-ligands **L1**, **L2** and **L3**.

**Table S2.** Summary of Crystal and Refinement Data for Pro-ligands **L1**, **L2** and **L3**.

**Table S3.** Summary of Crystal and Refinement Data for Complexes **Sc-1**, **Sc-3** and **Sc-4**.

**Table S4.** Summary of Crystal and Refinement Data for Complex **Y-2**.

**Figure S6.**  $^1\text{H}$  NMR spectrum (500MHz, tol- $d_8$ , 298 K) of  $\{\text{ONNO}^{\text{Cum},\text{Me}}\}\text{H}_2$  (**L1**).

**Figure S7.**  $^{13}\text{C}\{^1\text{H}\}$  NMR spectrum (125 MHz, tol- $d_8$ , 298 K) of  $\{\text{ONNO}^{\text{Cum},\text{Me}}\}\text{H}_2$  (**L1**).

**Figure S8.**  $^1\text{H}$  NMR spectrum (500 MHz,  $\text{CDCl}_3$ , 298 K) of  $\{\text{ONOO}^{\text{Cum},\text{Me}}\}\text{H}_2$  (**L2**).

**Figure S9.**  $^{13}\text{C}\{\text{H}\}$  NMR spectrum (125 MHz,  $\text{CDCl}_3$ , 298 K) of  $\{\text{ONOO}^{\text{Cum},\text{Me}}\}\text{H}_2$  (**L2**).

**Figure S10.**  $^1\text{H}$  NMR spectrum (400 MHz,  $\text{CDCl}_3$ , 298 K) of  $\{\text{ONOO}^{\text{CumCl},\text{Me}}\}\text{H}_2$  (**L3**).

**Figure S11.**  $^{13}\text{C}\{\text{H}\}$  NMR spectrum (100 MHz,  $\text{CDCl}_3$ , 298 K) of  $\{\text{ONOO}^{\text{CumCl},\text{Me}}\}\text{H}_2(\text{L3})$ .

**Figure S12.**  $^1\text{H}$  NMR spectrum (400 MHz,  $\text{C}_6\text{D}_6$ , 338 K) of  $\text{Sc}\{\text{ONNO}^{\text{Cum},\text{Me}}\}(\text{N}(\text{SiHMe}_2)_2)$  (**Sc-1**).

**Figure S13.**  $^{13}\text{C}\{\text{H}\}$  NMR spectrum (100 MHz,  $\text{C}_6\text{D}_6$ , 338 K) of  $\text{Sc}\{\text{ONNO}^{\text{Cum},\text{Me}}\}(\text{N}(\text{SiHMe}_2)_2)$  (**Sc-1**).

**Figure S14.**  $^{29}\text{Si}\{\text{H}\}$  NMR spectrum (79 MHz,  $\text{C}_6\text{D}_6$ , 338 K) of  $\text{Sc}\{\text{ONNO}^{\text{Cum},\text{Me}}\}(\text{N}(\text{SiHMe}_2)_2)$  (**Sc-1**).

**Figure S15.**  $^{29}\text{Si}$  NMR spectrum (79 MHz,  $\text{C}_6\text{D}_6$ , 338 K) of  $\text{Sc}\{\text{ONNO}^{\text{Cum},\text{Me}}\}(\text{N}(\text{SiHMe}_2)_2)$  (**Sc-1**).

**Figure S16.**  $^1\text{H}$  NMR spectrum (500 MHz,  $\text{C}_6\text{D}_6$ , 298 K) of  $\text{Sc}\{\text{ONOO}^{\text{Cum},\text{Me}}\}(\text{N}(\text{SiHMe}_2)_2)$  (**Sc-2**).

**Figure S17.**  $^{13}\text{C}\{\text{H}\}$  NMR spectrum (125 MHz,  $\text{C}_6\text{D}_6$ , 298 K) of  $\text{Sc}\{\text{ONOO}^{\text{Cum},\text{Me}}\}(\text{N}(\text{SiHMe}_2)_2)$  (**Sc-2**).

**Figure S18.**  $^1\text{H}$  NMR spectrum (400 MHz,  $\text{C}_6\text{D}_6$ , 298 K) of  $\text{Sc}\{\text{ONOO}^{\text{CumCl},\text{Me}}\}(\text{N}(\text{SiHMe}_2)_2)$  (**Sc-3**).

**Figure S19.**  $^{13}\text{C}\{\text{H}\}$  NMR spectrum (100 MHz,  $\text{C}_6\text{D}_6$ , 298 K) of  $\text{Sc}\{\text{ONOO}^{\text{CumCl},\text{Me}}\}(\text{N}(\text{SiHMe}_2)_2)$  (**Sc-3**).

**Figure S20.**  $^{29}\text{Si}\{\text{H}\}$  NMR spectrum (79 MHz,  $\text{C}_6\text{D}_6$ , 298 K) of  $\text{Sc}\{\text{ONOO}^{\text{CumCl},\text{Me}}\}(\text{N}(\text{SiHMe}_2)_2)$  (**Sc-3**).

**Figure S21.**  $^{29}\text{Si}$  NMR spectrum (79 MHz,  $\text{C}_6\text{D}_6$ , 298 K) of  $\text{Sc}\{\text{ONOO}^{\text{CumCl},\text{Me}}\}(\text{N}(\text{SiHMe}_2)_2)$  (**Sc-3**).

**Figure S22.**  $^1\text{H}$  NMR spectrum (400 MHz,  $\text{C}_6\text{D}_6$ , 333 K) of  $\text{Sc}\{\text{ONOO}^{\text{Cum},\text{Cum}}\}(\text{N}(\text{SiHMe}_2)_2)$  (**Sc-4**).

**Figure S23.**  $^{13}\text{C}\{\text{H}\}$  NMR spectrum (100 MHz,  $\text{C}_6\text{D}_6$ , 333 K) of  $\text{Sc}\{\text{ONOO}^{\text{Cum,Cum}}\}(\text{N}(\text{SiHMe}_2)_2)$  (**Sc-4**).

**Figure S24.**  $^{29}\text{Si}\{\text{H}\}$  NMR spectrum (79 MHz,  $\text{C}_6\text{D}_6$ , 333 K) of  $\text{Sc}\{\text{ONOO}^{\text{Cum,Cum}}\}(\text{N}(\text{SiHMe}_2)_2)$  (**Sc-4**).

**Figure S25.**  $^{29}\text{Si}$  NMR spectrum (79 MHz,  $\text{C}_6\text{D}_6$ , 333 K) of  $\text{Sc}\{\text{ONOO}^{\text{Cum,Cum}}\}(\text{N}(\text{SiHMe}_2)_2)$  (**Sc-4**).

**Figure S26.**  $^1\text{H}$  NMR spectrum (400 MHz,  $\text{C}_6\text{D}_6$ , 313 K) of  $\text{Y}\{\text{ONNO}^{\text{Cum},\text{Me}}\}(\text{N}(\text{SiHMe}_2)_2)$  (**Y-1**).

**Figure S27.**  $^{13}\text{C}$  NMR spectrum (100 MHz,  $\text{C}_6\text{D}_6$ , 313 K) of  $\text{Y}\{\text{ONNO}^{\text{Cum},\text{Me}}\}(\text{N}(\text{SiHMe}_2)_2)$  (**Y-1**)

**Figure S28.**  $^1\text{H}$  NMR spectrum (500 MHz,  $\text{C}_6\text{D}_6$ , 313 K) of  $\text{Y}\{\text{ONOO}^{\text{Cum},\text{Me}}\}(\text{N}(\text{SiHMe}_2)_2)$  (**Y-2**).

**Figure S29.**  $^{13}\text{C}$  NMR spectrum (125 MHz,  $\text{C}_6\text{D}_6$ , 313 K) of  $\text{Y}\{\text{ONOO}^{\text{Cum},\text{Me}}\}(\text{N}(\text{SiHMe}_2)_2)$  (**Y-2**).

**Figure S30.**  $^{29}\text{Si}\{\text{H}\}$  NMR spectrum (79 MHz,  $\text{C}_6\text{D}_6$ , 313 K) of  $\text{Y}\{\text{ONOO}^{\text{Cum},\text{Me}}\}(\text{N}(\text{SiHMe}_2)_2)$  (**Y-2**).

**Figure S31.**  $^{29}\text{Si}$  NMR spectrum (79 MHz,  $\text{C}_6\text{D}_6$ , 313 K) of  $\text{Y}\{\text{ONOO}^{\text{Cum},\text{Me}}\}(\text{N}(\text{SiHMe}_2)_2)$  (**Y-2**).

**Figure S32.**  $^1\text{H}$  NMR spectrum (400 MHz,  $\text{C}_6\text{D}_6$ , 333 K) of  $\text{Y}\{\text{ONOO}^{\text{CumCl},\text{Me}}\}(\text{N}(\text{SiHMe}_2)_2)$  (**Y-3**).

**Figure S33.**  $^{13}\text{C}\{\text{H}\}$  NMR spectrum (100 MHz,  $\text{C}_6\text{D}_6$ , 333 K) of  $\text{Y}\{\text{ONOO}^{\text{CumCl},\text{Me}}\}(\text{N}(\text{SiHMe}_2)_2)$  (**Y-3**).

**Figure S34.**  $^{29}\text{Si}\{\text{H}\}$  NMR spectrum (79 MHz,  $\text{C}_6\text{D}_6$ , 333 K) of  $\text{Y}\{\text{ONOO}^{\text{CumCl},\text{Me}}\}(\text{N}(\text{SiHMe}_2)_2)$  (**Y-3**).

**Figure S35.**  $^{29}\text{Si}$  NMR spectrum (79 MHz,  $\text{C}_6\text{D}_6$ , 333 K) of  $\text{Y}\{\text{ONOO}^{\text{CumCl},\text{Me}}\}(\text{N}(\text{SiHMe}_2)_2)$  (Y-3).

**Figure S36.** Detail of the homo-decoupled methine region of the  $^1\text{H}$  NMR spectrum (500 MHz,  $\text{CDCl}_3$ , 298 K) of a PLA produced from the **Sc-1/iPrOH** (1:1) system in toluene ( $P_r = 0.77$ ) (Table 2, entry 5).

**Figure S37.** Detail of the homo-decoupled methine region of the  $^1\text{H}$  NMR spectrum (500 MHz,  $\text{CDCl}_3$ , 298 K) of a PLA produced from the **Sc-3/iPrOH** (1:1) system in toluene ( $P_r = 0.80$ ) (Table 2, entry 12).

**Figure S38.** MALDI-TOF mass spectrum (main population:  $\text{Na}^+$ ; minor population:  $\text{K}^+$ ) of a PLA produced from the **Sc-3/iPrOH** (1:1) system in toluene ( $P_r = 0.80$ ) (Table 2, entry 12).

**Figure S39.** Detail of the homo-decoupled methine region of the  $^1\text{H}$  NMR spectrum (500 MHz,  $\text{CDCl}_3$ , 298 K) of a PLA produced from the **Sc-4/iPrOH** (1:1) system in toluene ( $P_r = 0.83$ ) (Table 2, entry 15).

**Figure S40.** Detail of the methylene region of the  $^{13}\text{C}\{^1\text{H}\}$  NMR spectrum (125 MHz,  $\text{CDCl}_3$ , 298 K) of a PHB produced from the **Y-1** system in toluene ( $P_r = 0.81$ ) (Table 3, entry 33).

**Figure S41.** Detail of the methylene region of the  $^{13}\text{C}\{^1\text{H}\}$  NMR spectrum (125 MHz,  $\text{CDCl}_3$ , 298 K) of a PHB produced from the **Y-3/iPrOH** (1:1) system in toluene ( $P_r = 0.87$ ) (Table 3, entry 36).

## Crystal structures of pro-ligands L1, L2 and L3

X-ray diffraction analyses revealed that pro-ligands  $\{\text{ONNO}^{\text{Cum},\text{Me}}\}\text{H}_2$  (**L1**),  $\{\text{ONOO}^{\text{Cum},\text{Me}}\}\text{H}_2$  (**L2**) and  $\{\text{ONOO}^{\text{CumCl},\text{Me}}\}\text{H}_2$  (**L3**) are structurally very similar (Figure S1). Crystallographic data and structural determination details are summarized in Table S2, and important bond distances and angles are given in Table S1. The C–N distances (1.4744(14)-1.489(3) Å) in these three compounds are typical of amino-phenols and compare well in particular with those of the identical pro-ligands described above.<sup>1</sup> The C–O(1), C–O(2) and C–N(1) bond distances and the C–N(1)–C, C–O(1)–H and C–O(2)–H bond angles are similar in the three compounds and fall within the expected ranges for such molecules.<sup>1</sup>

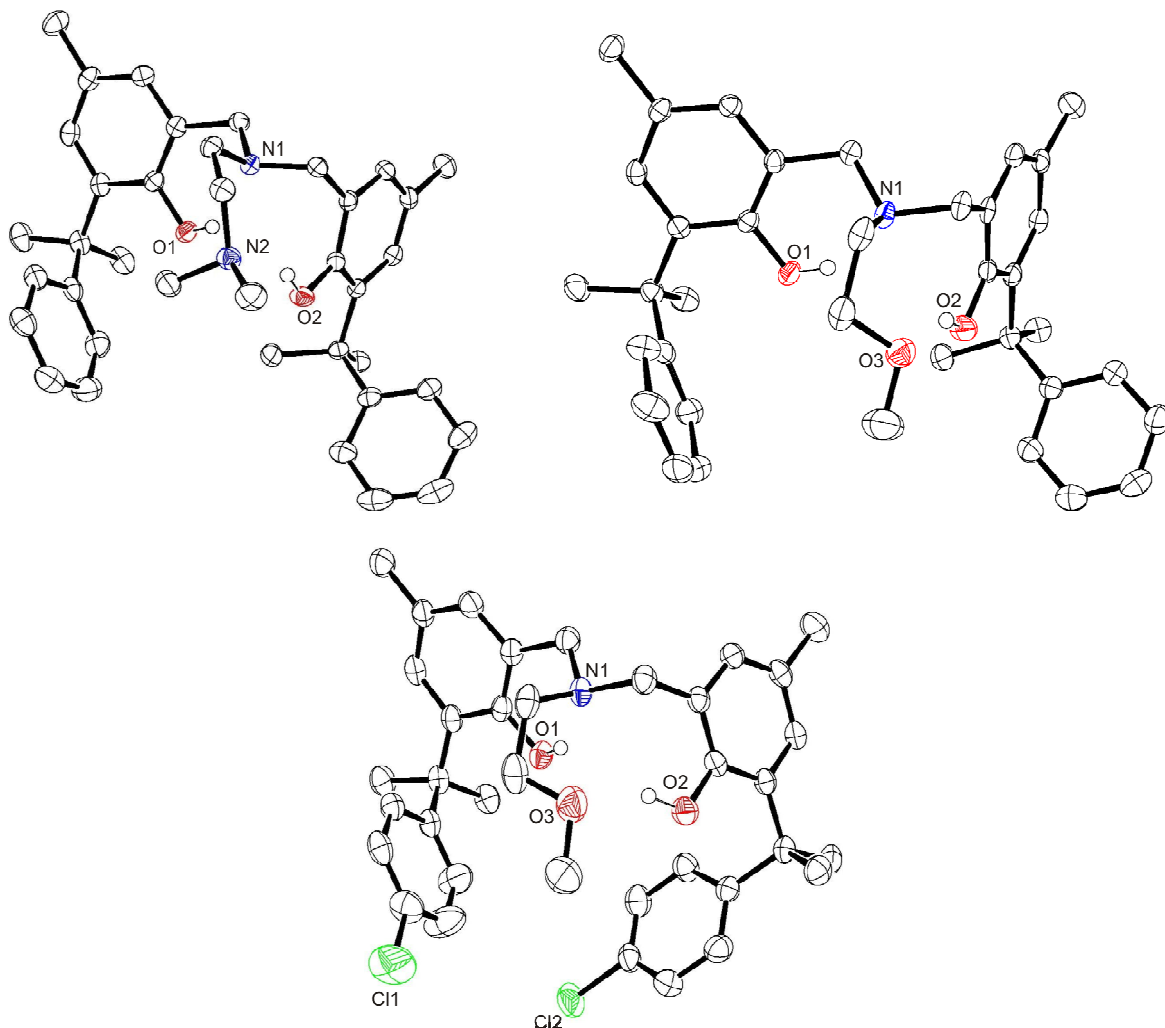


**Figure S1.** Solid-state molecular structures of  $\{\text{ONNO}^{\text{Cum},\text{Me}}\}\text{H}_2$  (**L1**– top left),  $\{\text{ONOO}^{\text{Cum},\text{Me}}\}\text{H}_2$  (**L2**– top right) and  $\{\text{ONOO}^{\text{CumCl},\text{Me}}\}\text{H}_2$  (**L3**– bottom). All hydrogen atoms are omitted for clarity except those of the OH groups.

**Table S1.** Selected bond distances ( $\text{\AA}$ ) and angles (deg) for pro-ligands **L1**, **L2** and **L3**.

	<b>L1</b>	<b>L2</b>	<b>L3</b>
C–N(1)	1.4744(14)	1.4760(17)	1.489(3)
C–O(1)	1.3734(14)	1.3691(16)	1.368(2)
C–O(2)	1.3669(13)	1.3697(17)	1.370(3)
O(1)–H	0.82	0.84	0.91(3)
O(2)–H	0.82	0.84	0.80(3)
C–N(1)–C	110.06(9)	110.03(11)	109.12(17)
C–O(1)–H	109.5	109.5	111.0(16)
C–O(2)–H	109.5	109.5	106.7(19)

(1) Cai C.-X., Amgoune A., Lehmann C. W., Carpentier J.-F. *Chem. Comm.* **2004**, 330; Amgoune A., Thomas C.M., Roisnel T., Carpentier J.-F. *Chem. Eur. J.* **2004**, 12, 169; Bouyahyi M., Ajellal N., Kirillov E., Thomas C. M., Carpentier J.-F. *Chem. Eur. J.* **2011**, 17, 1872.

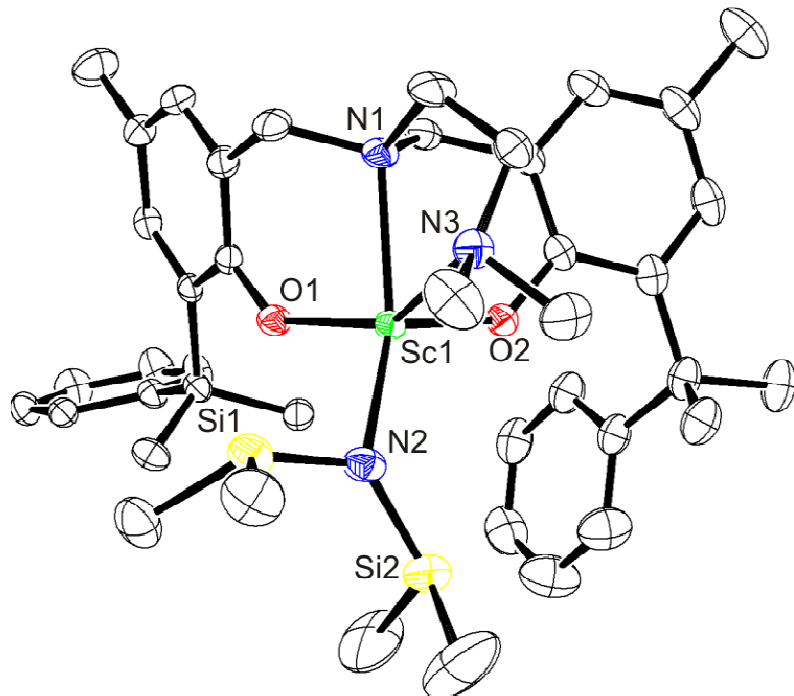


**Figure S2.** Solid-state molecular structure of  $\text{Sc}\{\text{ONNO}^{\text{Cum},\text{Me}}\}(\text{N}(\text{SiHMe}_2)_2)$  (**Sc-1**). All hydrogen atoms are omitted for clarity; thermal ellipsoids drawn at the 50% probability.

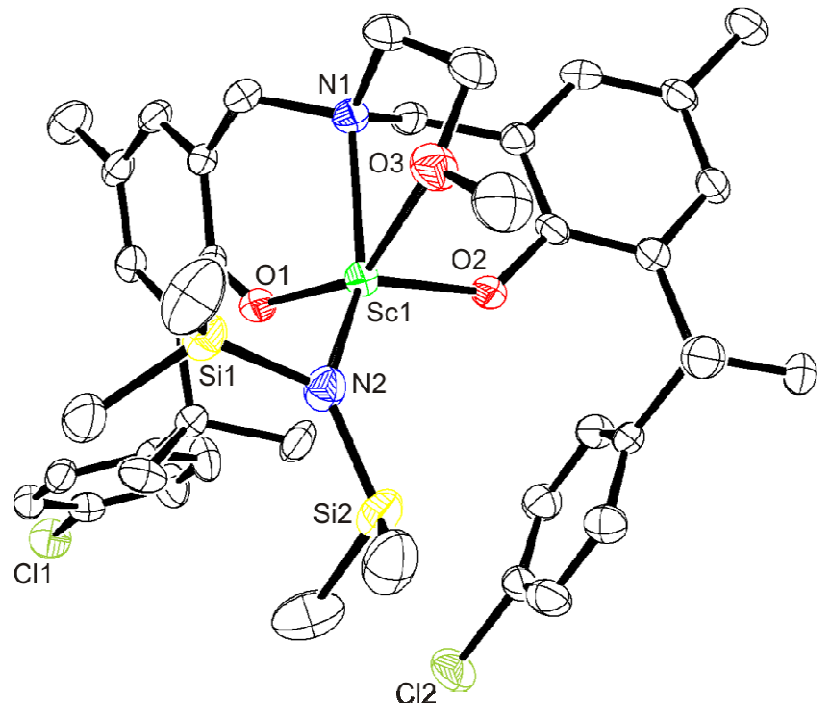


**Figure S3.** Solid-state molecular structure of  $\text{Sc}\{\text{ONOO}^{\text{CumCl},\text{Me}}\}(\text{N}(\text{SiHMe}_2)_2)$  (**Sc-3**). All hydrogen atoms are omitted for clarity; thermal ellipsoids drawn at the 50% probability.

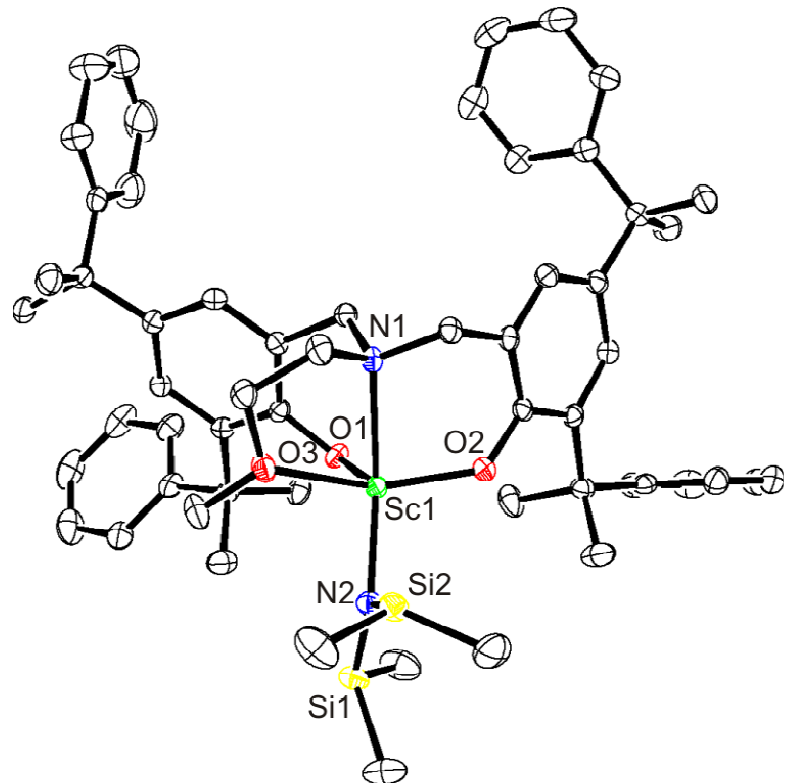


**Figure S4.** Solid-state molecular structure of  $\text{Sc}\{\text{ONOO}^{\text{Cum,Cum}}\}(\text{N}(\text{SiHMe}_2)_2)$  (**Sc-4**). All hydrogen atoms are omitted for clarity; thermal ellipsoids drawn at the 50% probability.

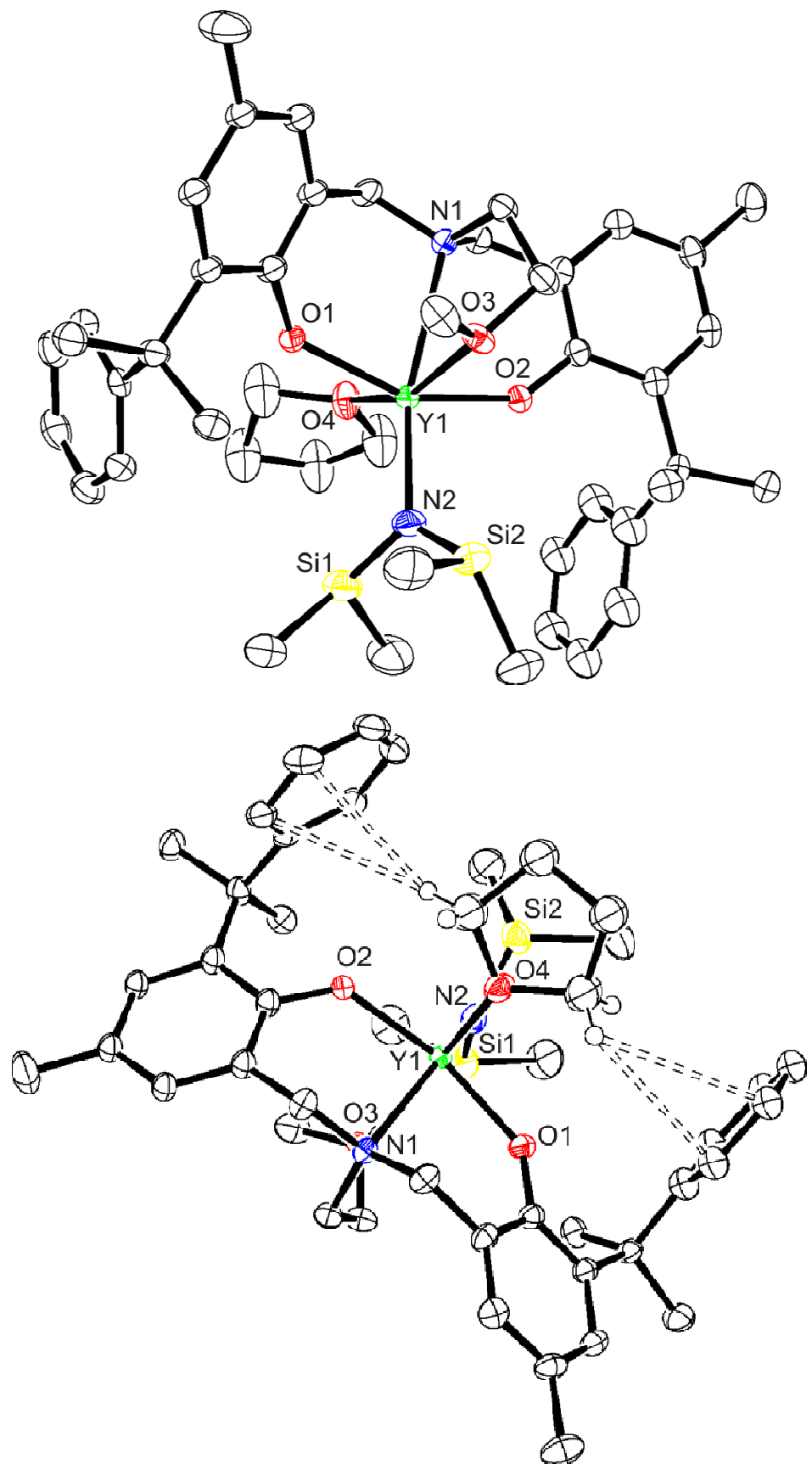


**Figure S5.** Solid-state molecular structure of  $\text{Y}\{\text{ONOO}^{\text{Cum},\text{Me}}\}(\text{N}(\text{SiHMe}_2)_2)\text{THF}$  (**Y-2**). All hydrogen atoms are omitted for clarity; thermal ellipsoids drawn at the 50% probability.

**Table S2.** Summary of Crystal and Refinement Data for Pro-ligands **L1**, **L2** and **L4**.

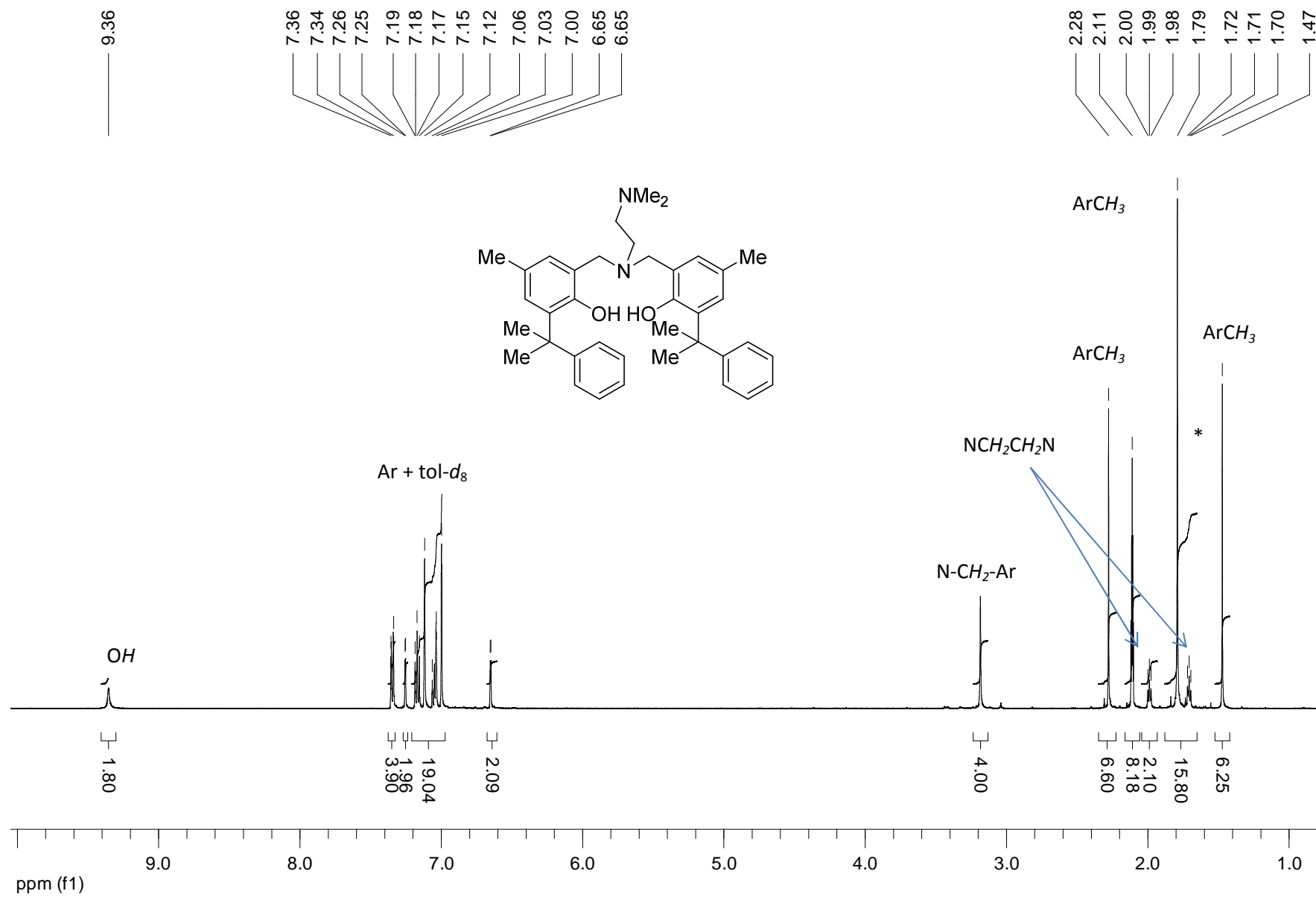
	{ONNO <sup>Cum,Me</sup> }H <sub>2</sub> ( <b>L1</b> )	{ONOO <sup>Cum,Me</sup> }H <sub>2</sub> ( <b>L2</b> )	{ONOO <sup>CumCl,Me</sup> }H <sub>2</sub> ( <b>L3</b> )
Empirical formula	C <sub>38</sub> H <sub>48</sub> N <sub>2</sub> O <sub>2</sub>	C <sub>37</sub> H <sub>45</sub> NO <sub>3</sub>	C <sub>37</sub> H <sub>43</sub> Cl <sub>2</sub> NO <sub>3</sub>
Formula weight	564.78	551.74	620.62
Crystal system	Triclinic	Monoclinic	Monoclinic
Space group	P -1	P 2 <sub>1</sub> /c	P 2 <sub>1</sub> / <i>c</i>
<i>a</i> , Å	9.5098(9)	13.4212(7)	12.9265(7)
<i>b</i> , Å	11.7992(11)	17.8521(9)	22.6950(11)
<i>c</i> , Å	14.6808(15)	13.6834(5)	12.5985(7)
$\alpha$ , deg	77.799(4)	90	90
$\beta$ , deg	86.607(4)	104.1090(10)	110.847(2)
$\gamma$ , deg	81.796(4)	90	90
Volume, Å <sup>3</sup>	1592.9(3)	3179.6(3)	3454.0(3)
<i>Z</i>	2	4	4
Density, g.m <sup>-3</sup>	1.178	1.153	1.193
Abs. coeff., mm <sup>-1</sup>	0.072	0.072	0.223
F(000)	612	1192	1320
Crystal size, mm	0.33 × 0.27 × 0.15 mm	0.42 × 0.27 × 0.08	0.29 × 0.16 × 0.08
θ range, deg	3.43 to 27.48	2.97 to 27.48	2.95 to 27.48
Limiting indices	-10 ≤ <i>h</i> ≤ 12, -15 ≤ <i>k</i> ≤ 14, -18 ≤ <i>l</i> ≤ 18	-17 ≤ <i>h</i> ≤ 17, -23 ≤ <i>k</i> ≤ 23, -12 ≤ <i>l</i> ≤ 17	-14 ≤ <i>h</i> ≤ 16, -20 ≤ <i>k</i> ≤ 29, -16 ≤ <i>l</i> ≤ 16
Reflec. Collected	24371	27662	29822
Reflec. Unique [I>2σ(I)]	7174 (6100)	7198 (5057)	7913 (4482)
Data/restrains/ param.	7174 / 0 / 389	7198 / 0 / 379	7913 / 0 / 401
Goodness-of-fit on F <sup>2</sup>	1.032	1.012	1.033
R <sub>1</sub> [ $>2\sigma(I)$ ] (all data)	0.0417 (0.0504)	0.045 (0.0732)	0.0581 (0.1087)
wR <sub>2</sub> [ $>2\sigma(I)$ ] (all data)	0.1064 (0.1132)	0.1058 (0.1212)	0.1343 (0.1521)
Largest diff., e.A <sup>-3</sup>	0.321 and -0.235	0.2 and -0.228	0.349 and -0.397

**Table S3.** Summary of Crystal and Refinement Data for Complexes **Sc-1**, **Sc-3** and **Sc-4**.

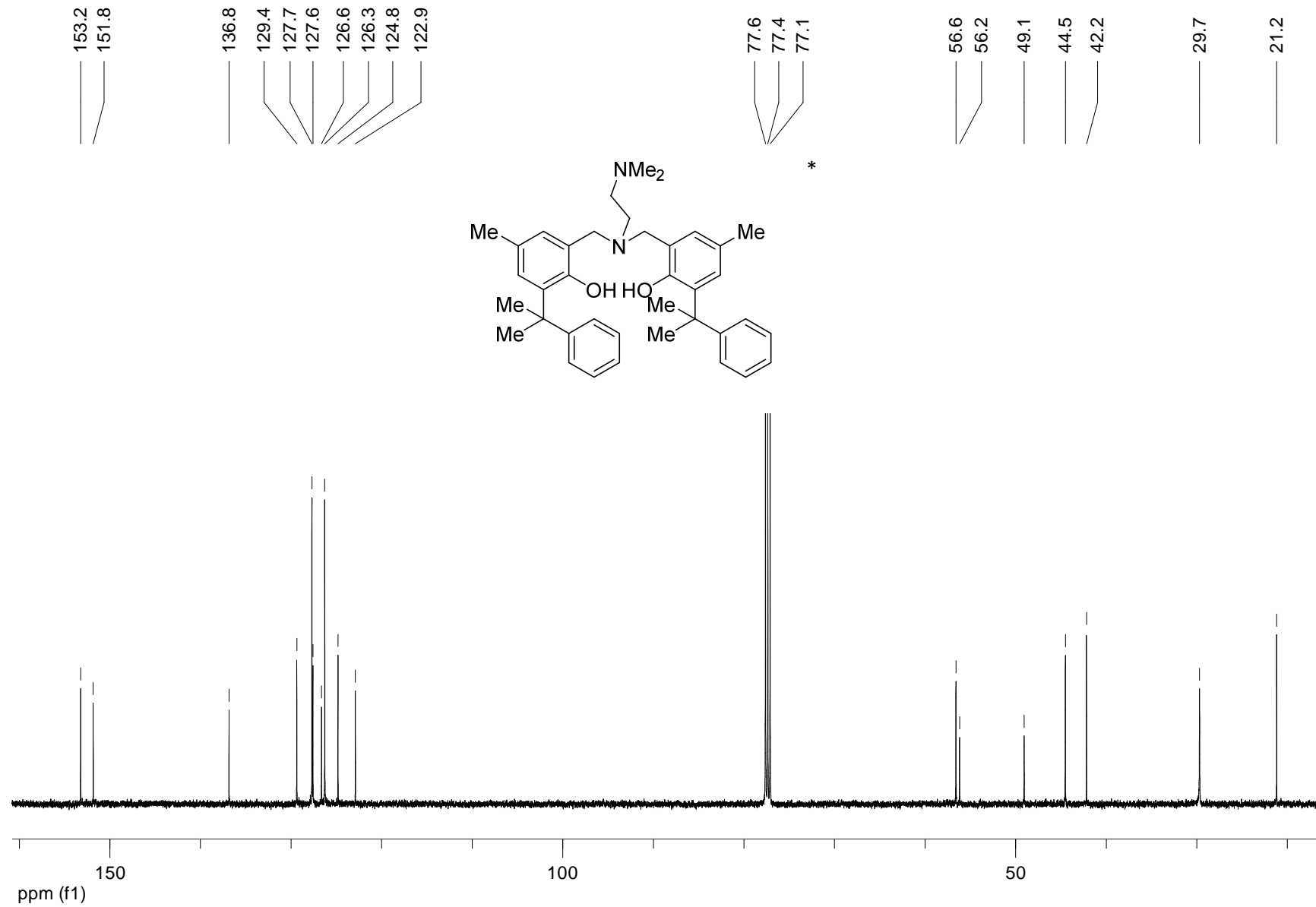
	Sc{ONNO <sup>Cum,Me</sup> } (N(SiHMe <sub>2</sub> ) <sub>2</sub> ) <b>(Sc-1)</b>	Sc{ONOOC <sup>CumCl,Me</sup> } (N(SiHMe <sub>2</sub> ) <sub>2</sub> ) <b>(Sc-3)</b>	Sc{ONOOC <sup>Cum,Cum</sup> } (N(SiHMe <sub>2</sub> ) <sub>2</sub> ) <b>(Sc-4)</b>
Empirical formula	C <sub>42</sub> H <sub>60</sub> N <sub>3</sub> O <sub>2</sub> ScSi <sub>2</sub>	C <sub>41</sub> H <sub>55</sub> Cl <sub>2</sub> N <sub>2</sub> O <sub>3</sub> ScSi <sub>2</sub>	C <sub>57</sub> H <sub>73</sub> N <sub>2</sub> O <sub>3</sub> ScSi <sub>2</sub>
Formula weight	740.07	795.91	935.31
Crystal system	Triclinic	Monoclinic	Monoclinic
Space group	P -1	P 2 <sub>1</sub> /c	P 2 <sub>1</sub> /n
<i>a</i> , Å	10.4197(3)	11.0295(3)	17.9067(6)
<i>b</i> , Å	13.9848(4)	28.6061(7)	11.2217(4)
<i>c</i> , Å	14.8410(3)	13.5365(5)	26.2238(8)
$\alpha$ , deg	84.6900(10)	90	90
$\beta$ , deg	85.6890(10)	99.707(2)	91.3950(10)
$\gamma$ , deg	82.7970(10)	90	90
Volume, Å <sup>3</sup>	2131.89(10)	4209.8(2)	5267.9(3)
<i>Z</i>	2	4	4
Density, g.m <sup>-3</sup>	1.153	1.256	1.179
Abs. coeff., mm <sup>-1</sup>	0.265	0.397	0.229
F(000)	796	1688	2008
Crystal size, mm	0.40 × 0.30 × 0.28	0.34 × 0.21 × 0.12	0.47 × 0.32 × 0.25
θ range, deg	2.94 to 27.48	2.97 to 27.47	2.91 to 27.48
Limiting indices	-13 ≤ <i>h</i> ≤ 13, -17 ≤ <i>k</i> ≤ 18, -19 ≤ <i>l</i> ≤ 19	-14 ≤ <i>h</i> ≤ 14, -37 ≤ <i>k</i> ≤ 27, -17 ≤ <i>l</i> ≤ 17	-23 ≤ <i>h</i> ≤ 21, -14 ≤ <i>k</i> ≤ 14, -30 ≤ <i>l</i> ≤ 34
Reflec. Collected	34295	34798	45053
Reflec. Unique [ <i>I</i> >2σ( <i>I</i> )]	9747 (7707)	9600 (7246)	12060 (9276)
Data/restrains/ param.	9747 / 0 / 479	9600 / 0 / 477	12060 / 0 / 605
Goodness-of-fit on F <sup>2</sup>	1.042	1.003	1.023
R <sub>1</sub> [ <i>I</i> >2σ( <i>I</i> )] (all data)	0.0442 (0.0593)	0.0554 (0.0809)	0.0437 (0.0633)
wR <sub>2</sub> [ <i>I</i> >2σ( <i>I</i> )] (all data)	0.1095 (0.1177)	0.1125 (0.1251)	0.102 (0.1117)
Largest diff., e.A <sup>-3</sup>	0.445 and -0.279	0.32 and -0.345	0.601 and -0.301

**Table S4.** Summary of Crystal and Refinement Data for Complex **Y-2**.

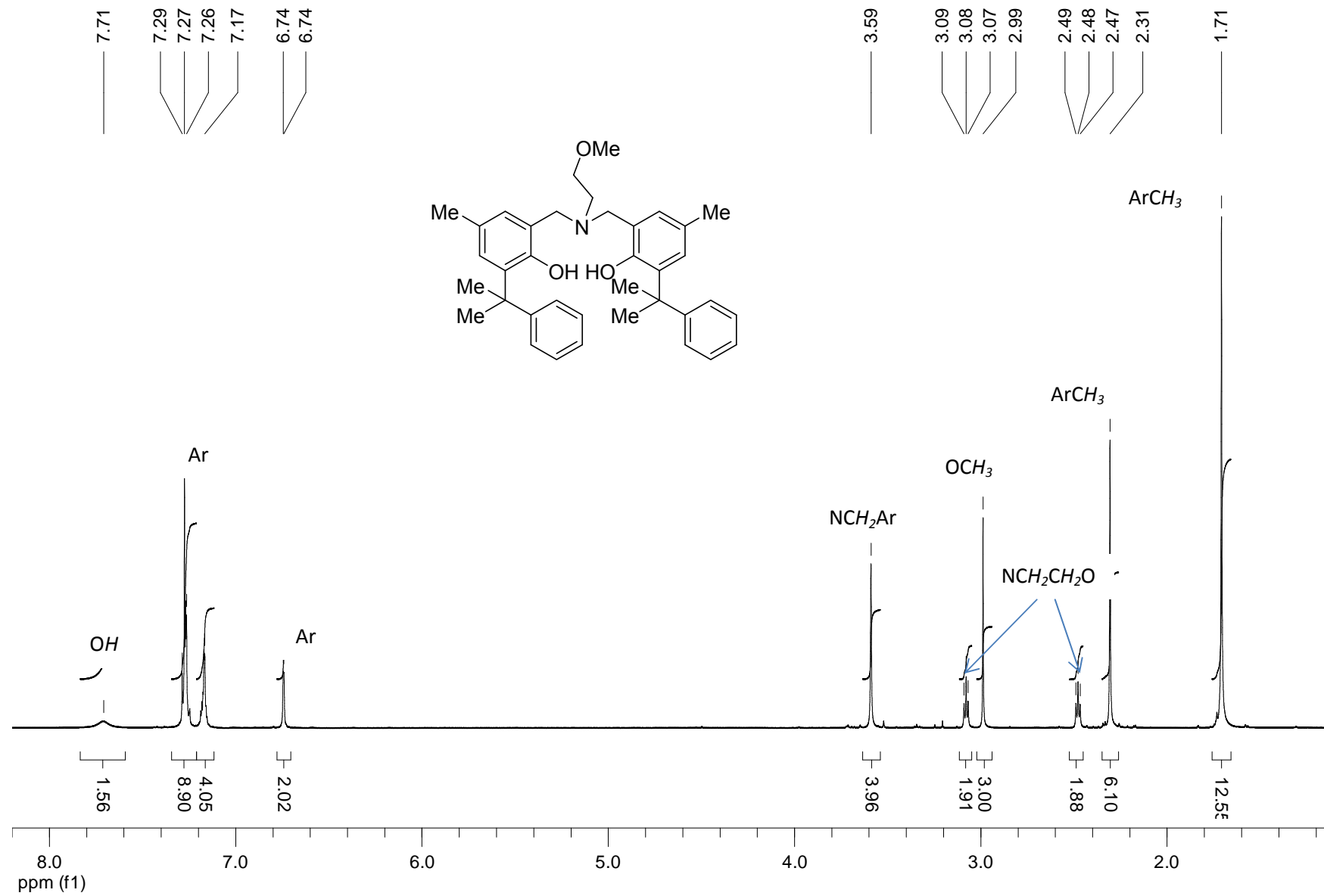
Y{ONOO <sup>Cum,Me</sup> } <sub>2</sub> (N(SiHMe <sub>2</sub> ) <sub>2</sub> )THF ( <b>Y-2</b> )	
Empirical formula	2(C <sub>45</sub> H <sub>65</sub> N <sub>2</sub> O <sub>4</sub> Si <sub>2</sub> Y)
Formula weight	1686.16
Crystal system	Triclinic
Space group	P -1
<i>a</i> , Å	11.8127(4)
<i>b</i> , Å	11.9689(3)
<i>c</i> , Å	36.3748(12)
$\alpha$ , deg	86.3270(10)
$\beta$ , deg	86.6490(10)
$\gamma$ , deg	62.0640(10)
Volume, Å <sup>3</sup>	4531.9(2)
Z	2
Density, g.m <sup>-3</sup>	1.236
Abs. coeff., mm <sup>-1</sup>	1.381
F(000)	1792
Crystal size, mm	0.37 × 0.33 × 0.17
$\theta$ range, deg	2.93 to 27.48
Limiting indices	$-15 \leq h \leq 15, -15 \leq k \leq 15,$ $-47 \leq l \leq 47$
Reflec. Collected	62991
Refle. Unique [I>2σ(I)]	20403 (14101)
Data/restrains/ param.	20403 / 0 / 870
Goodness-of-fit on F <sup>2</sup>	1.025
R <sub>1</sub> [I>2σ(I)] (all data)	0.0614 (0.1015)
wR <sub>2</sub> [I>2σ(I)] (all data)	0.1429 (0.1616)
Largest diff., e.A <sup>-3</sup>	1.592 and -1.635



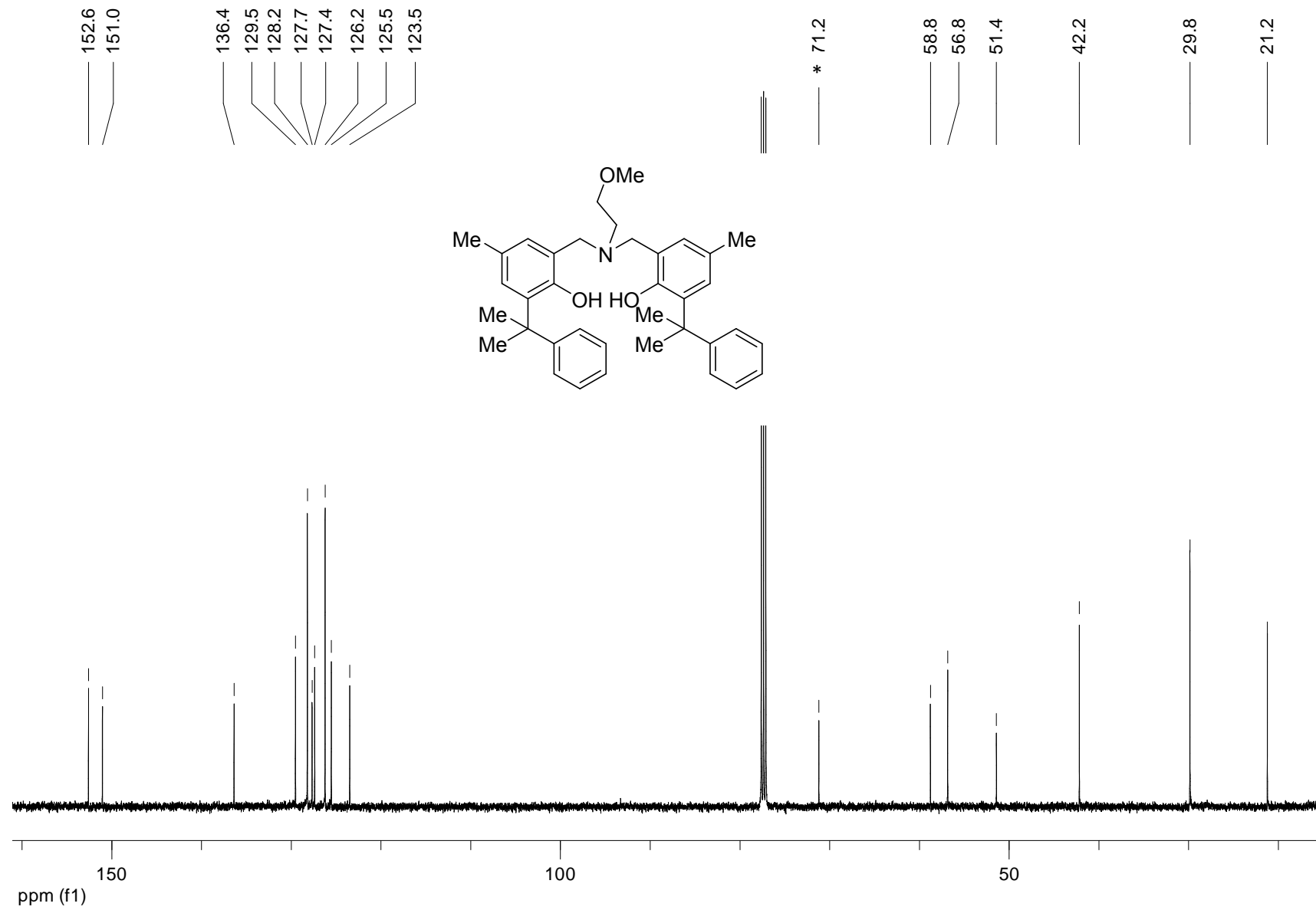
**Figure S6.**  $^1\text{H}$  NMR spectrum (500MHz,  $\text{tol}-d_8$ , 298 K) of  $\{\text{ONNO}^{\text{Cum},\text{Me}}\}\text{H}_2$  (**L1**). \* stands for solvent resonances.



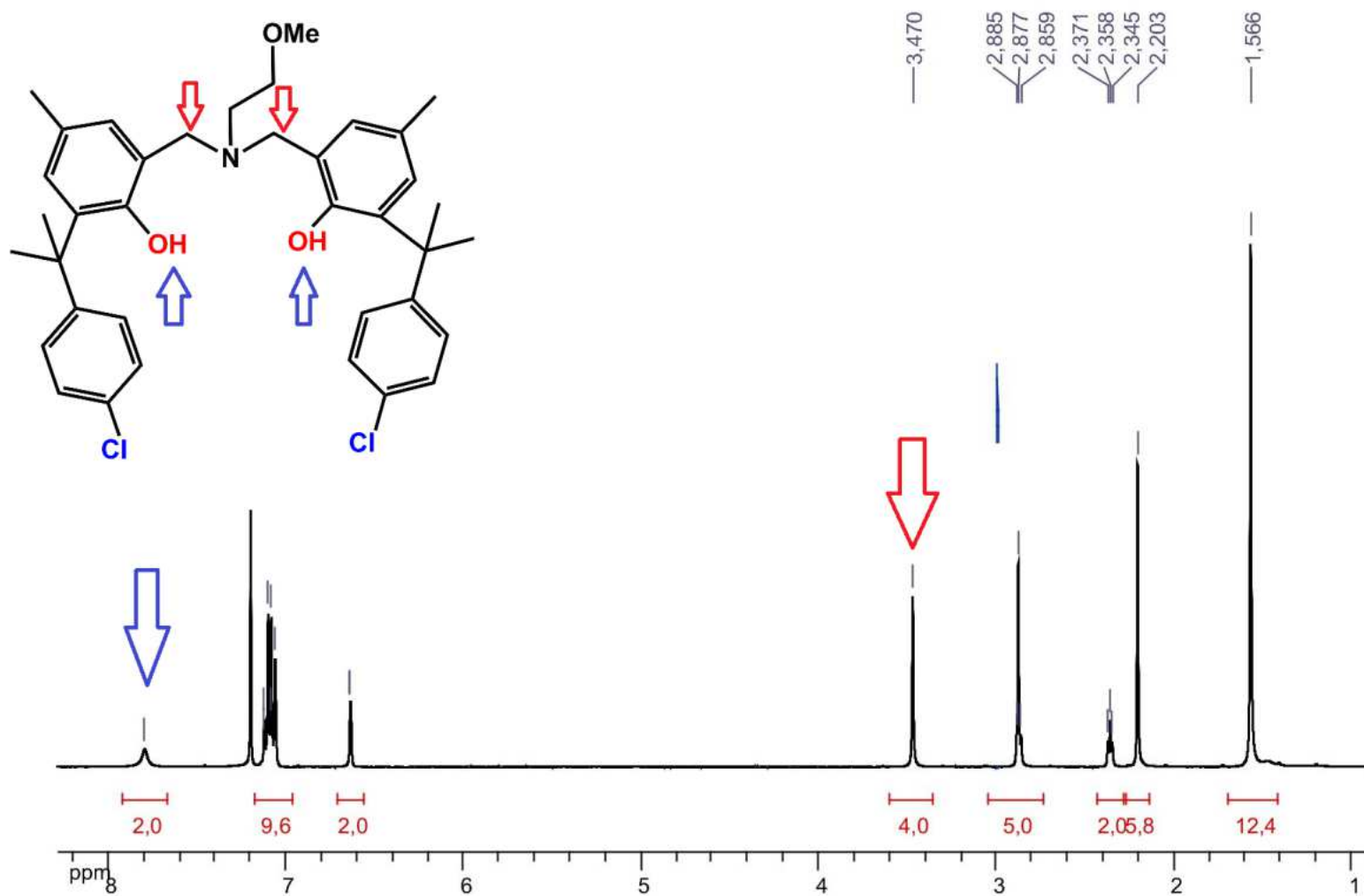
**Figure S7.**  $^{13}\text{C}\{^1\text{H}\}$  NMR spectrum (125 MHz,  $\text{CDCl}_3$ , 298 K) of  $\{\text{ONNO}^{\text{Cum},\text{Me}}\text{H}_2\}$  (**L1**). \* stands for solvent resonances.



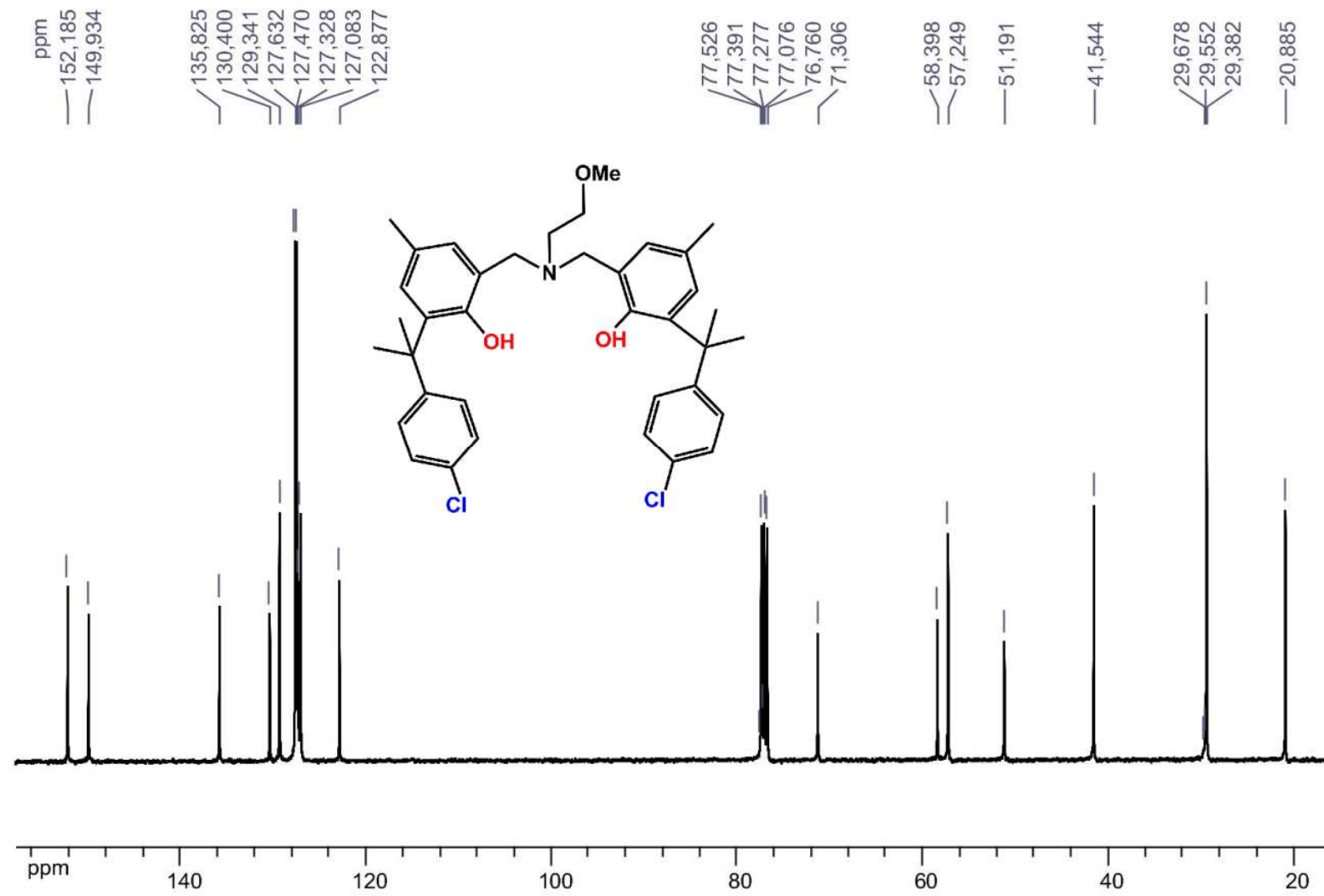
**Figure S8.**  $^1\text{H}$  NMR spectrum (500 MHz,  $\text{CDCl}_3$ , 298 K) of  $\{\text{ONOO}^{\text{Cum},\text{Me}}\}_2\text{H}_2$  (**L2**).



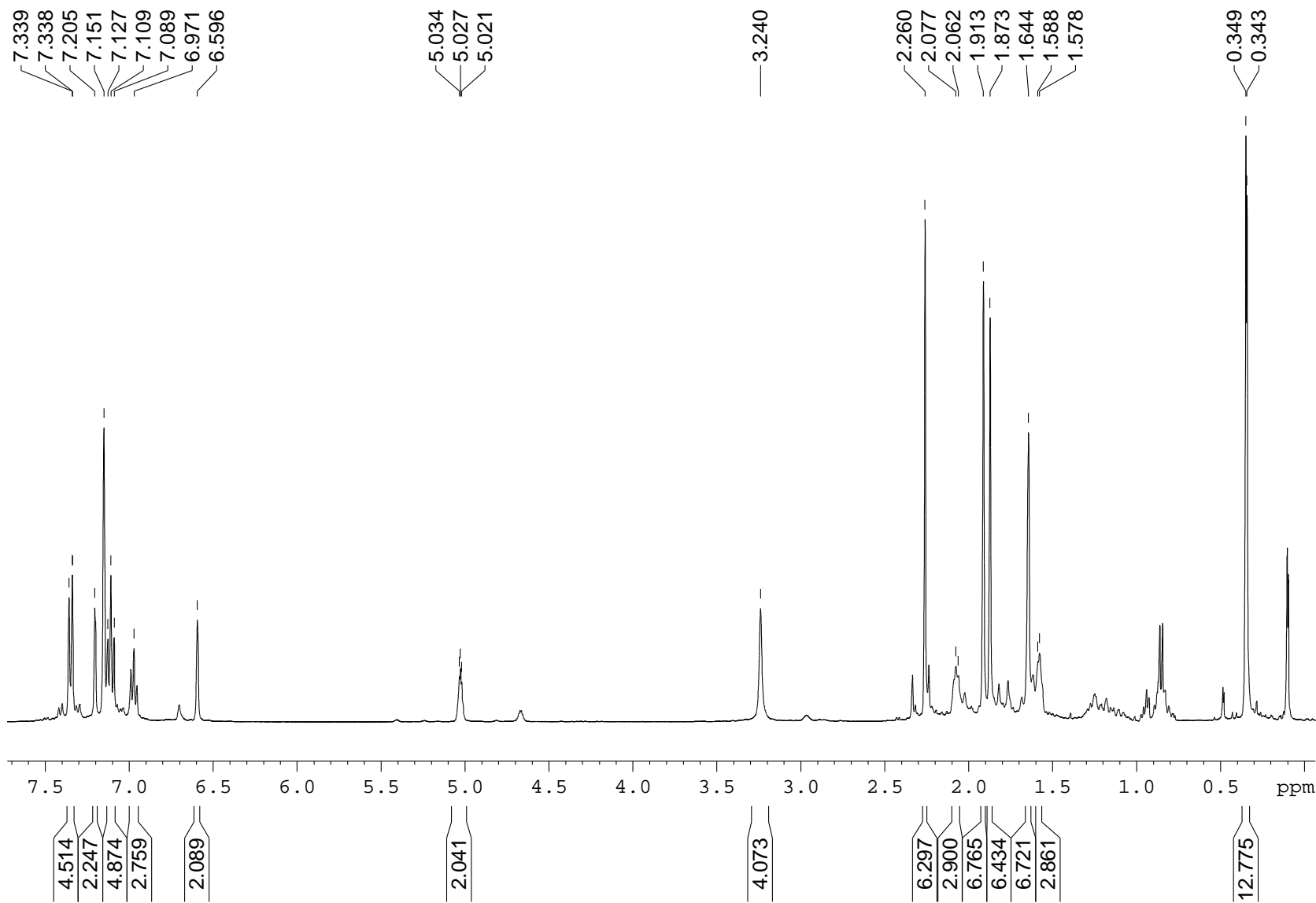
**Figure S9.**  $^{13}\text{C}\{\text{H}\}$  NMR spectrum (125 MHz,  $\text{CDCl}_3$ , 298 K) of  $\{\text{ONOO}^{\text{Cum},\text{Me}}\}\text{H}_2$  (**L2**). \* Stands for solvent resonances.



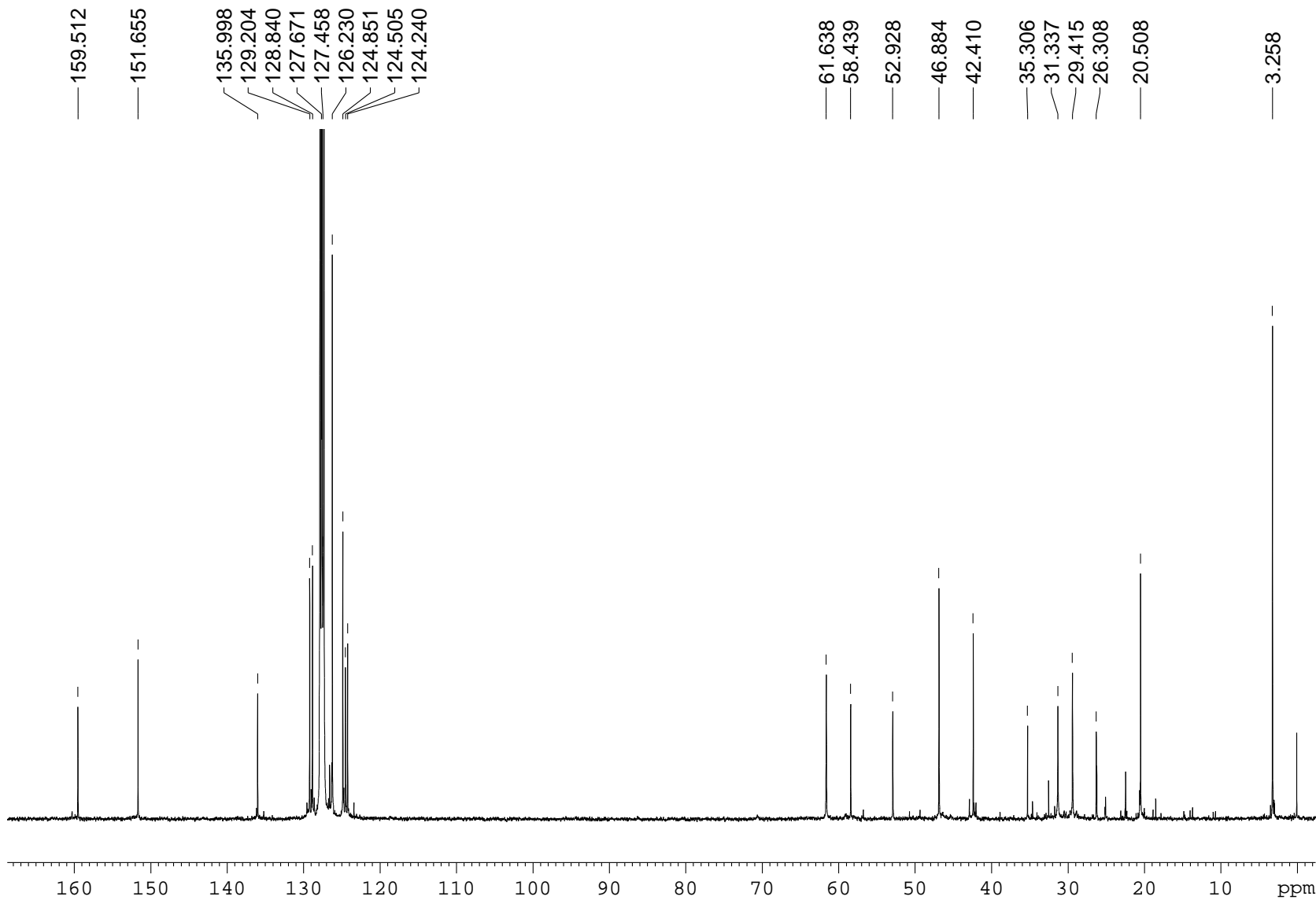
**Figure S10.**  $^1\text{H}$  NMR spectrum (400 MHz,  $\text{CDCl}_3$ , 298 K) of  $\{\text{ONOO}^{\text{CumCl},\text{Me}}\}_2$  (**L3**).



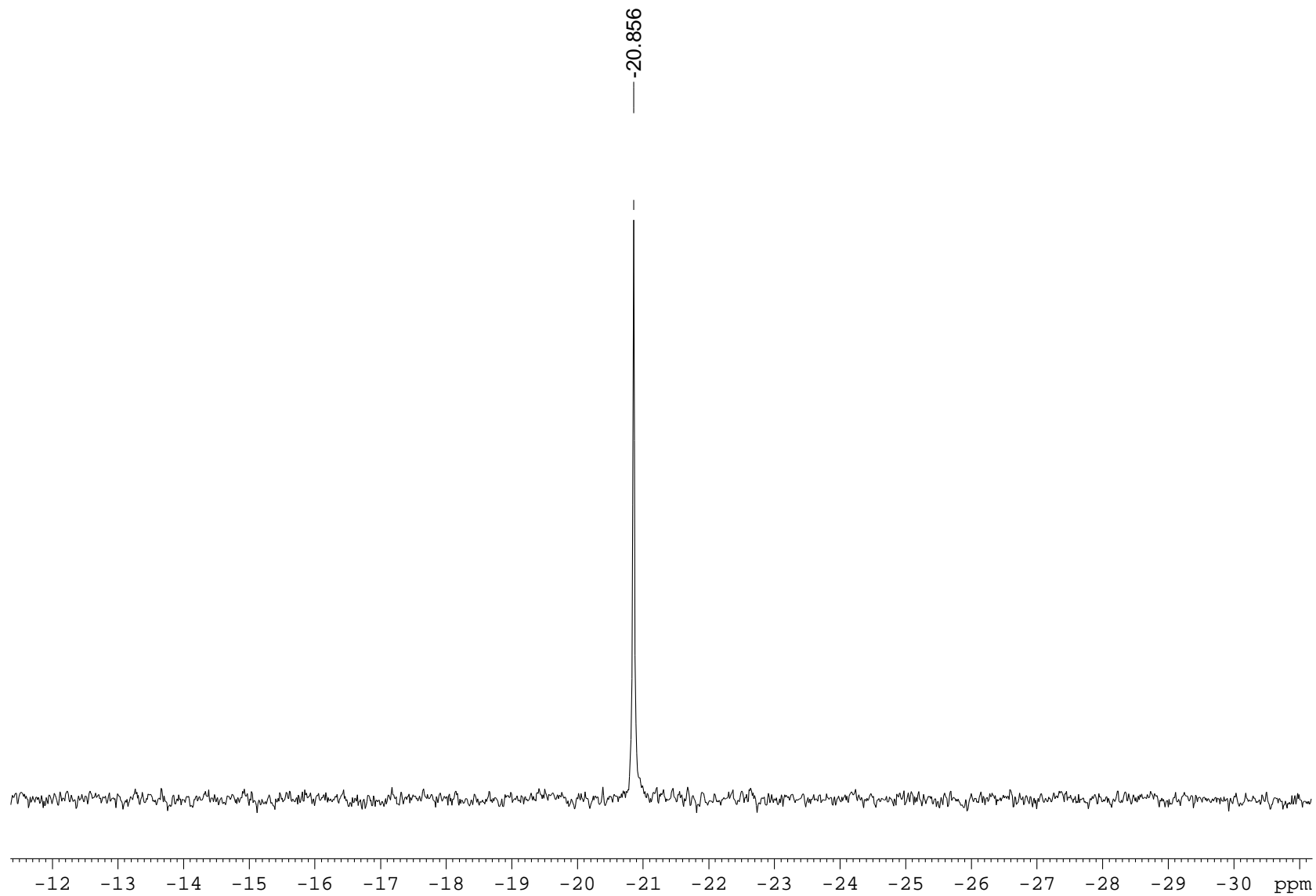
**Figure S11.**  $^{13}\text{C}\{\text{H}\}$  NMR spectrum (100 MHz,  $\text{CDCl}_3$ , 298 K) of  $\{\text{ONOO}^{\text{CumCl},\text{Me}}\}\text{H}_2$  (**L3**).



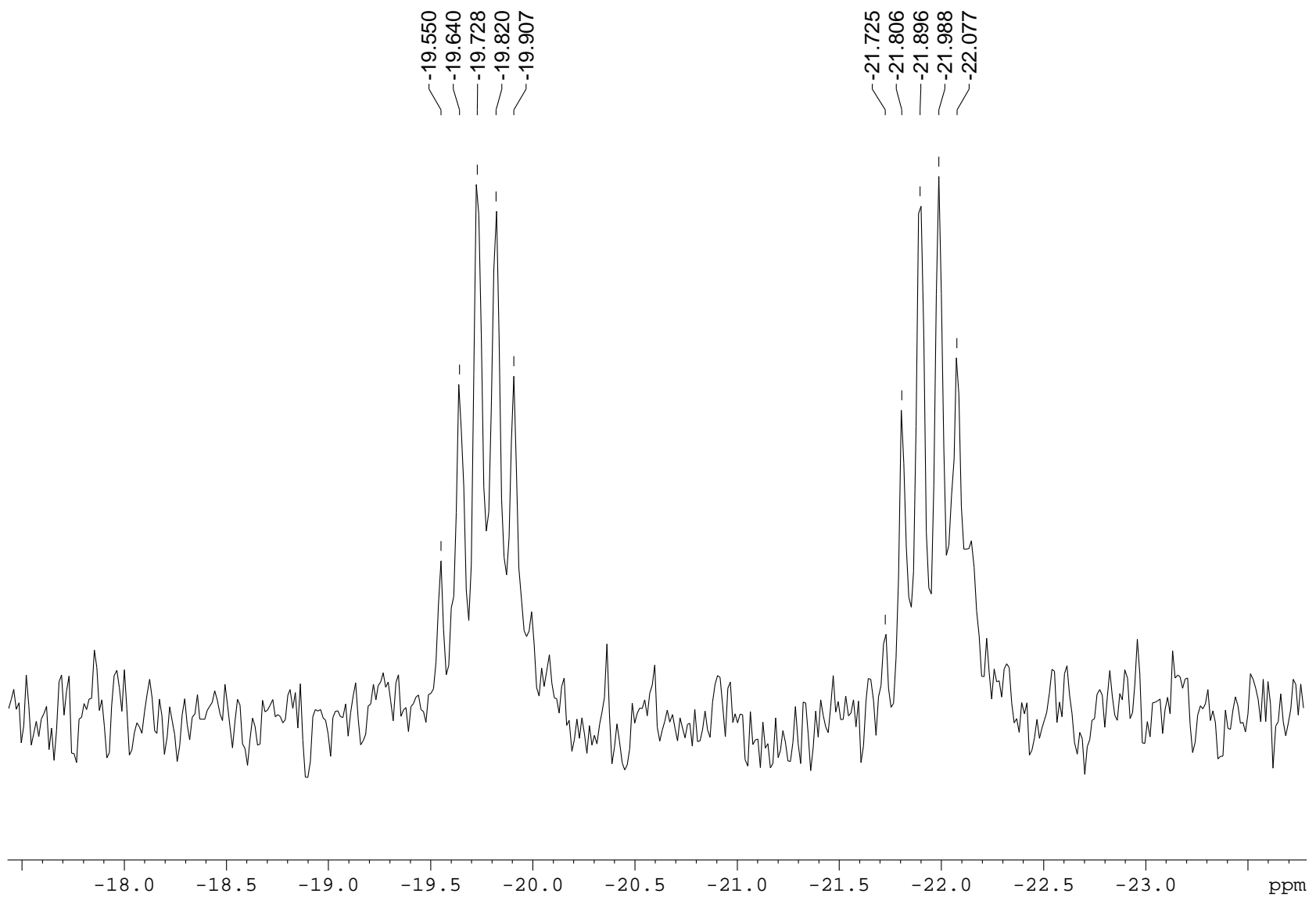
**Figure S12.** <sup>1</sup>H NMR spectrum (400 MHz, C<sub>6</sub>D<sub>6</sub>, 338 K) of Sc{ONNO<sup>Cum,Me</sup>} (N(SiHMe<sub>2</sub>)<sub>2</sub>) (**Sc-1**).



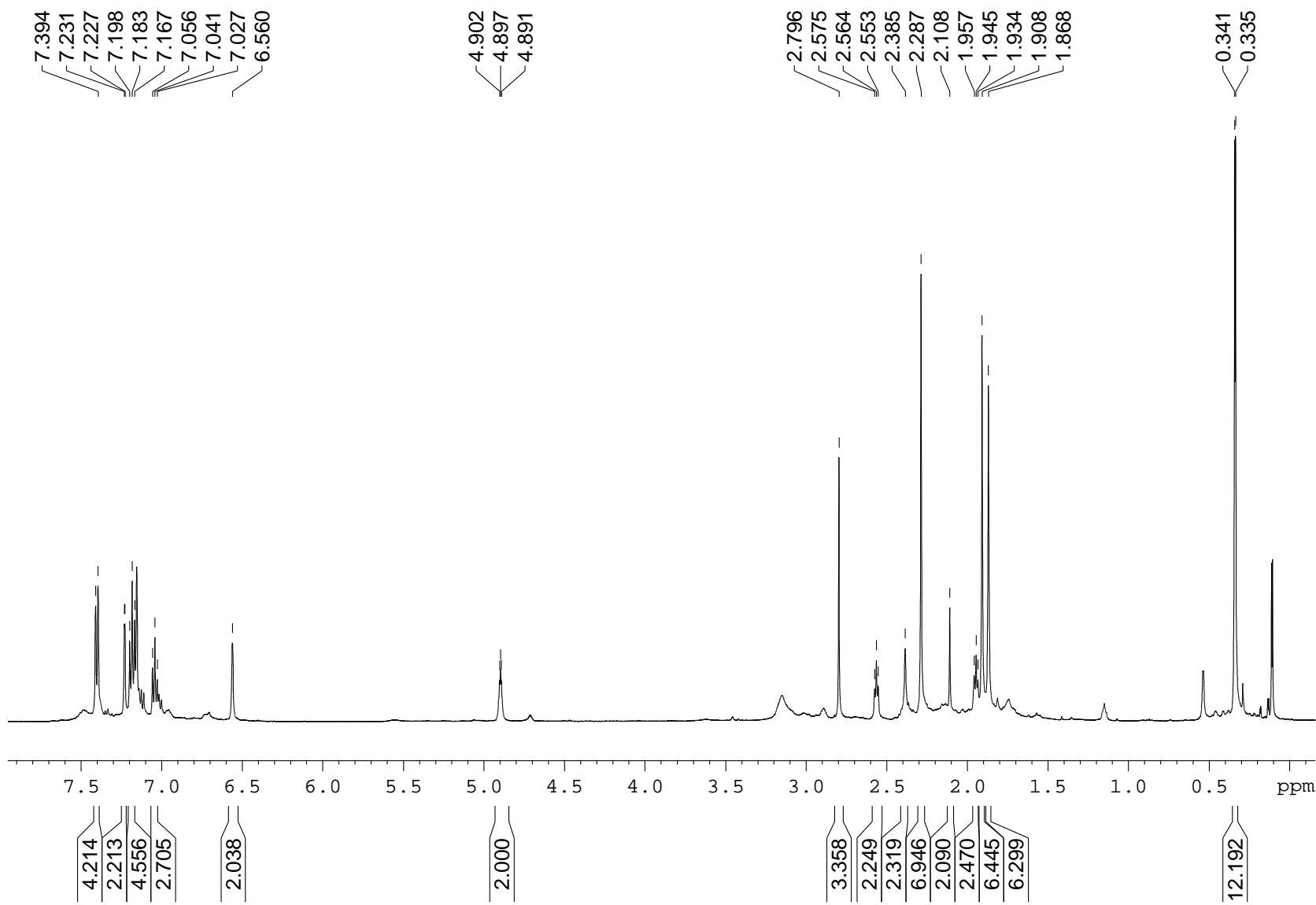
**Figure S13.**  $^{13}\text{C}\{\text{H}\}$  NMR spectrum (100 MHz,  $\text{C}_6\text{D}_6$ , 338 K) of  $\text{Sc}\{\text{ONNO}^{\text{Cum},\text{Me}}\}(\text{N}(\text{SiHMe}_2)_2)$  (**Sc-1**).



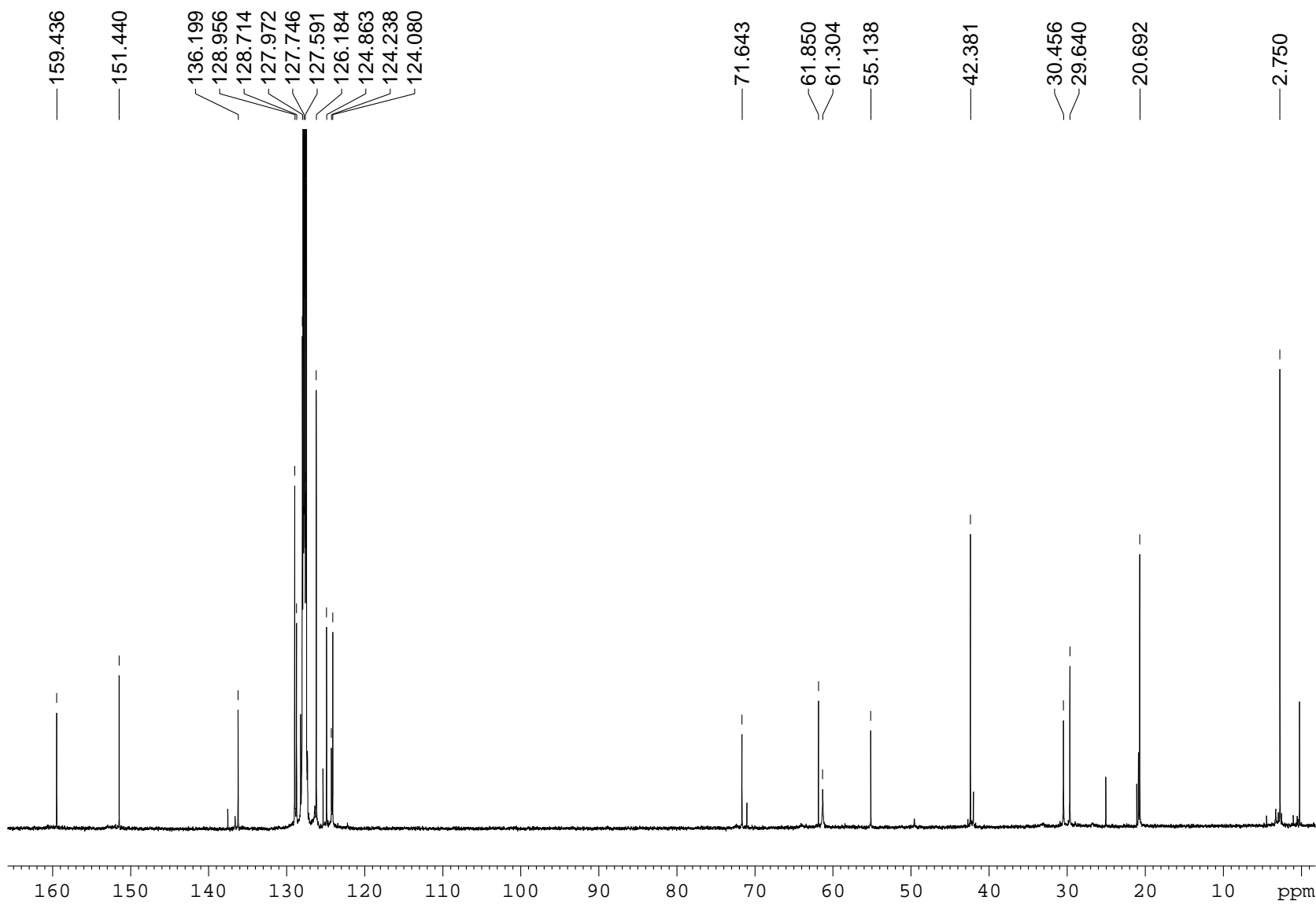
**Figure S14.**  $^{29}\text{Si}\{\text{H}\}$  NMR spectrum (79 MHz,  $\text{C}_6\text{D}_6$ , 338 K) of  $\text{Sc}\{\text{ONNO}^{\text{Cum},\text{Me}}\}(\text{N}(\text{SiHMe}_2)_2)$  (**Sc-1**).



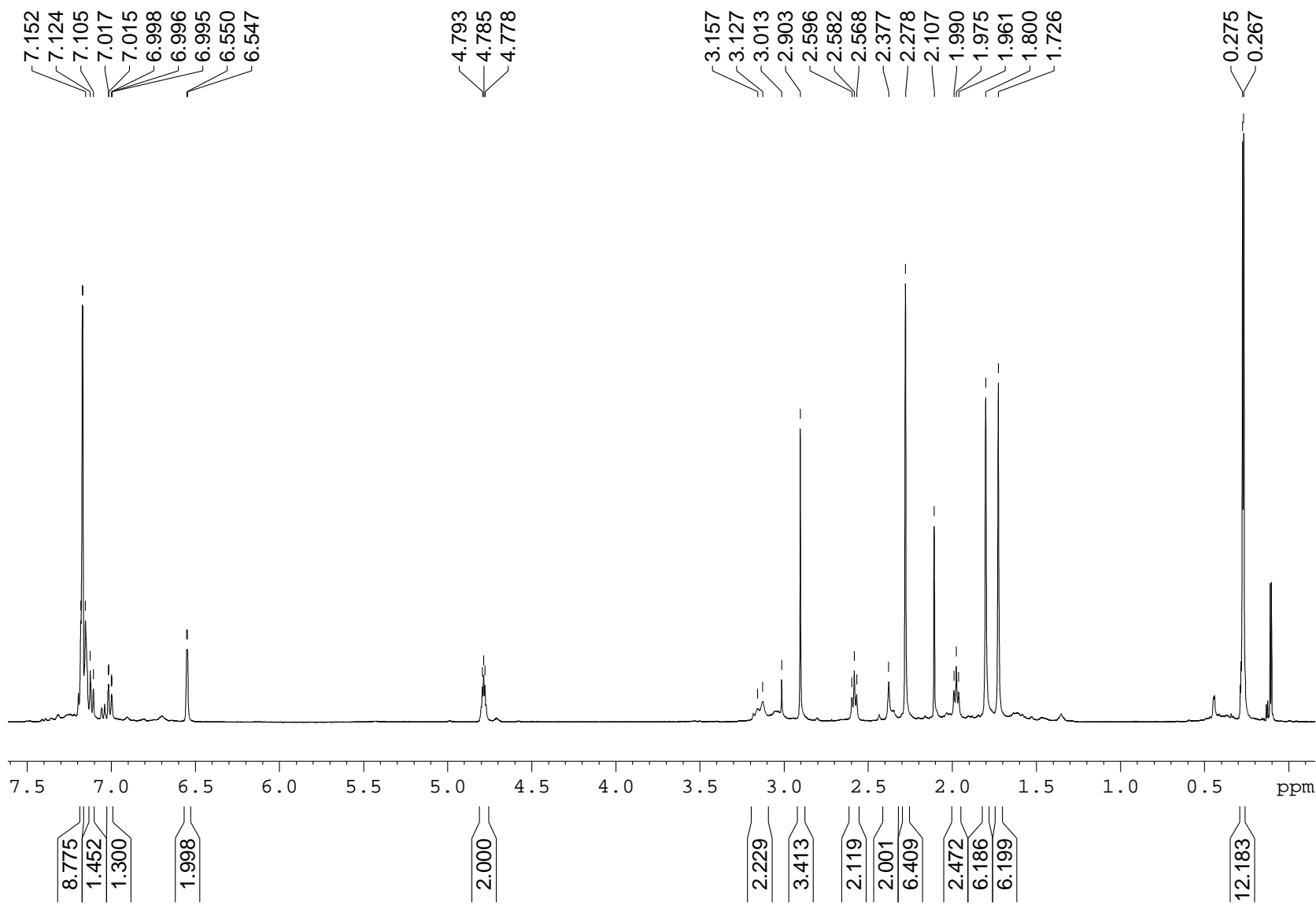
**Figure S15.**  $^{29}\text{Si}$  NMR spectrum (79 MHz,  $\text{C}_6\text{D}_6$ , 338 K) of  $\text{Sc}\{\text{ONNO}^{\text{Cum},\text{Me}}\}(\text{N}(\text{SiHMe}_2)_2)$  (**Sc-1**).



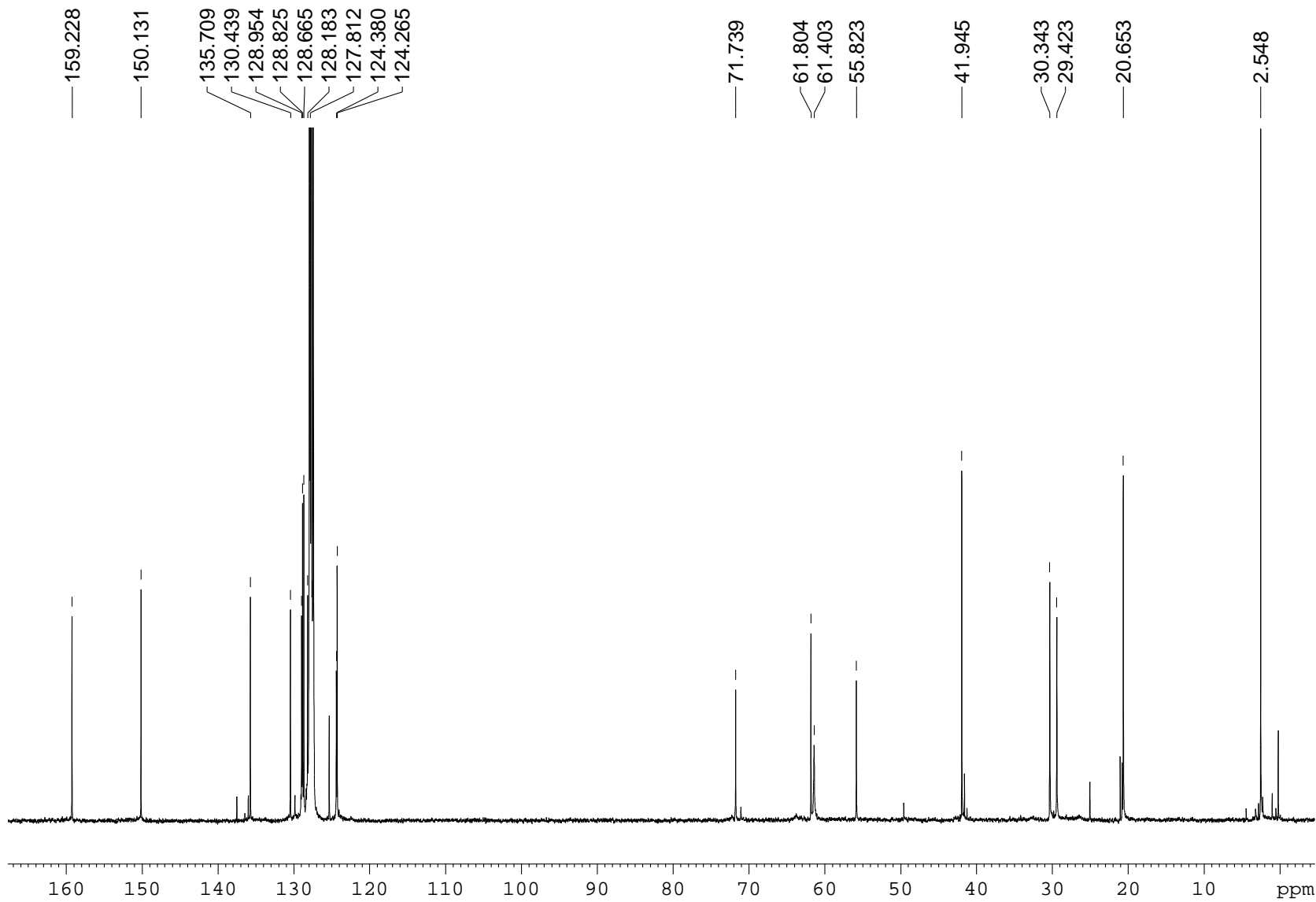
**Figure S16.** <sup>1</sup>H NMR spectrum (500 MHz, C<sub>6</sub>D<sub>6</sub>, 298 K) of Sc{ONOO<sup>Cum,Me</sup>}<sub>2</sub>(N(SiHMe<sub>2</sub>)<sub>2</sub>) (**Sc-2**).



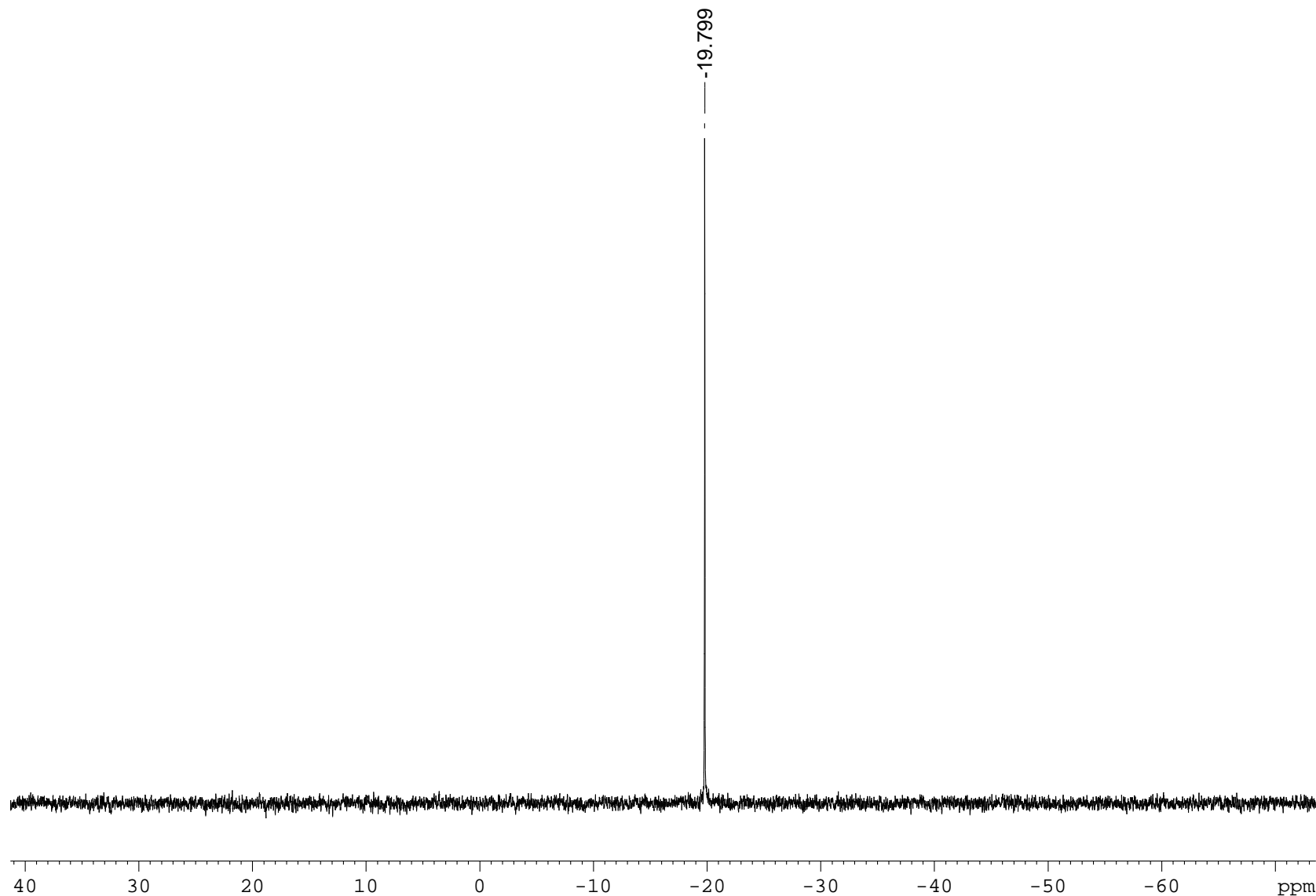
**Figure S17.**  $^{13}\text{C}\{\text{H}\}$  NMR spectrum (125 MHz,  $\text{C}_6\text{D}_6$ , 298 K) of  $\text{Sc}\{\text{ONOO}^{\text{Cum},\text{Me}}\}(\text{N}(\text{SiHMe}_2)_2)$  (**Sc-2**).



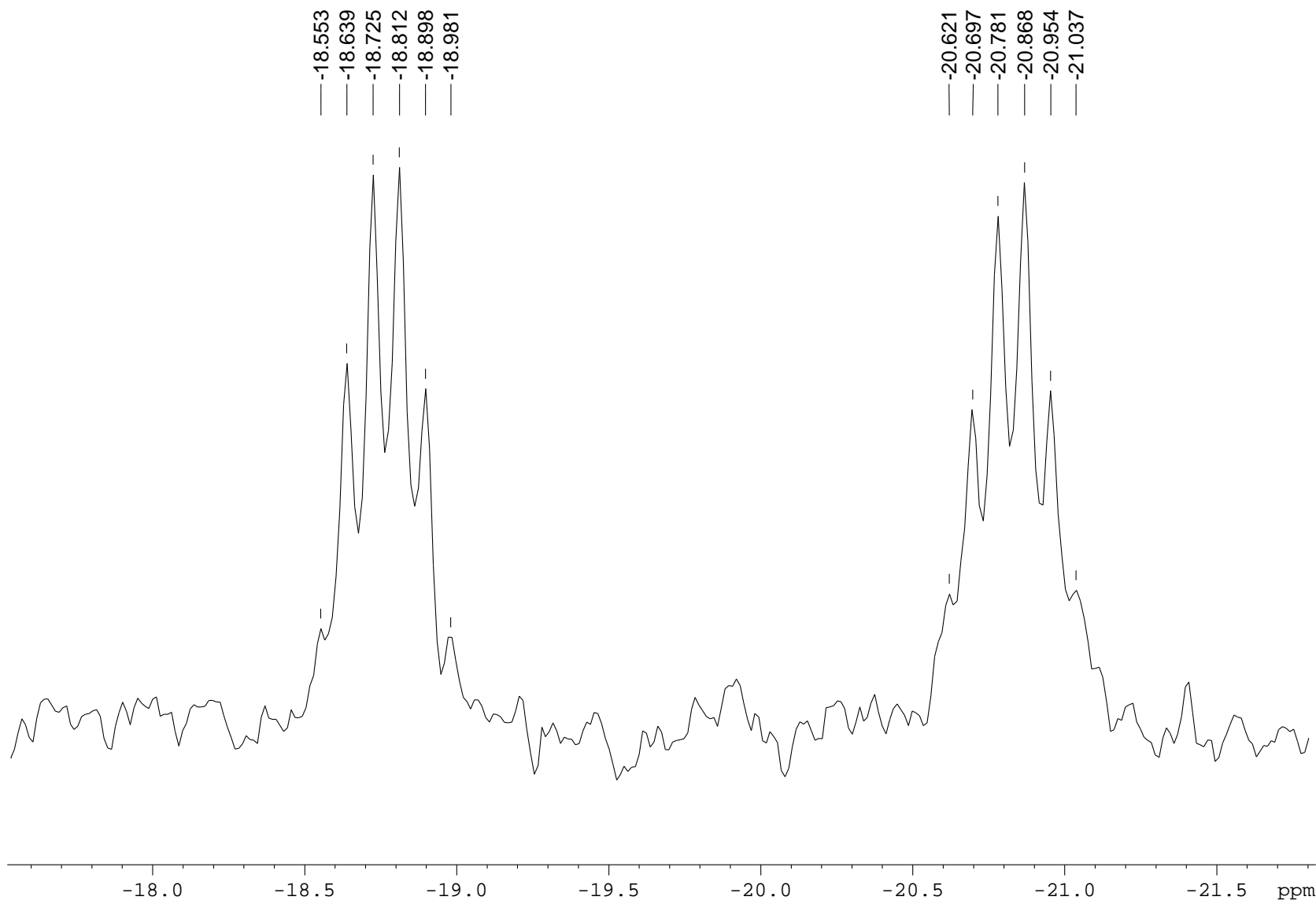
**Figure S18.**  $^1\text{H}$  NMR spectrum (400 MHz,  $\text{C}_6\text{D}_6$ , 298 K) of  $\text{Sc}\{\text{ONOO}^{\text{CumCl},\text{Me}}\}(\text{N}(\text{SiHMe}_2)_2)$  (**Sc-3**).



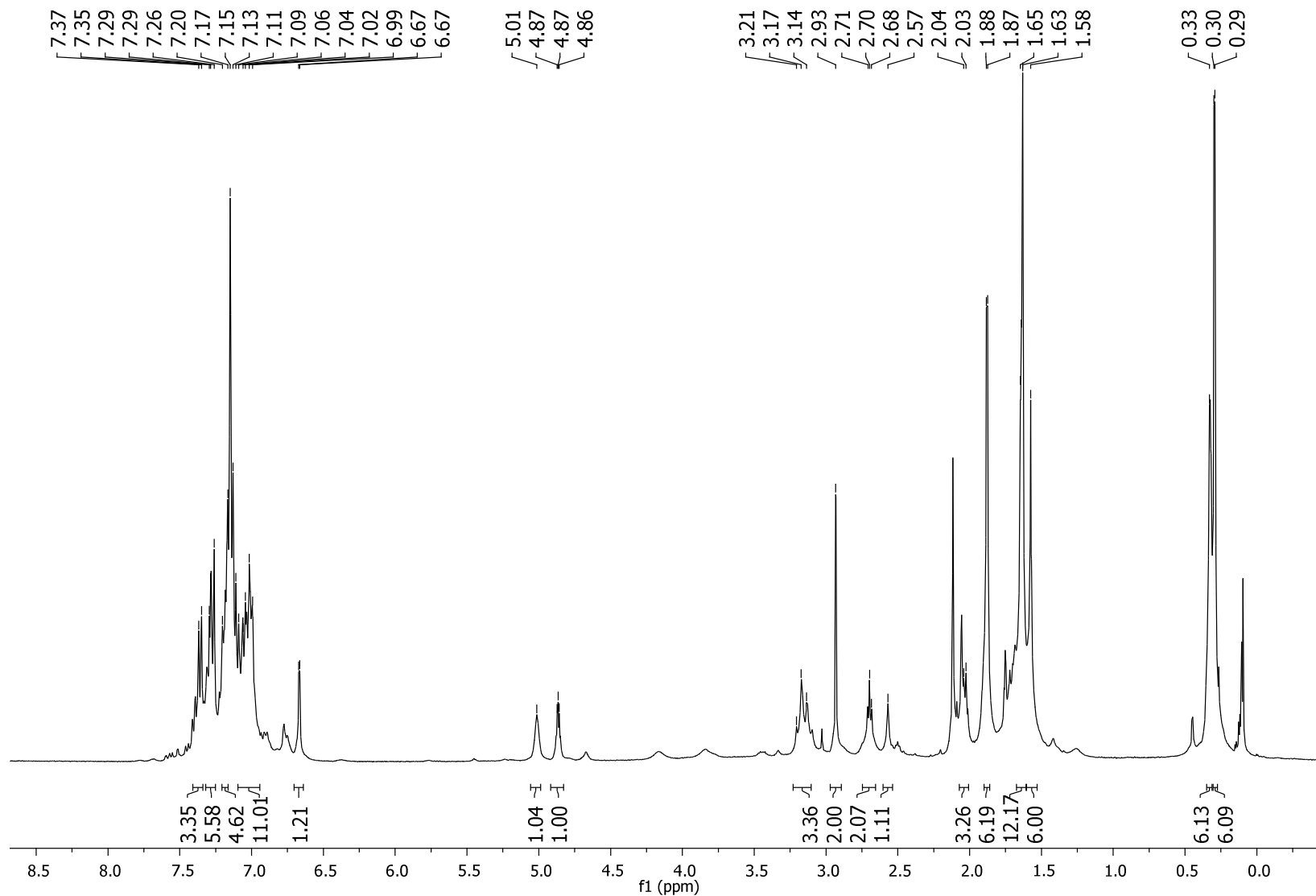
**Figure S19.**  $^{13}\text{C}\{\text{H}\}$  NMR spectrum (100 MHz,  $\text{C}_6\text{D}_6$ , 298 K) of  $\text{Sc}\{\text{ONOO}^{\text{CumCl},\text{Me}}\}(\text{N}(\text{SiHMe}_2)_2)$  (**Sc-3**).



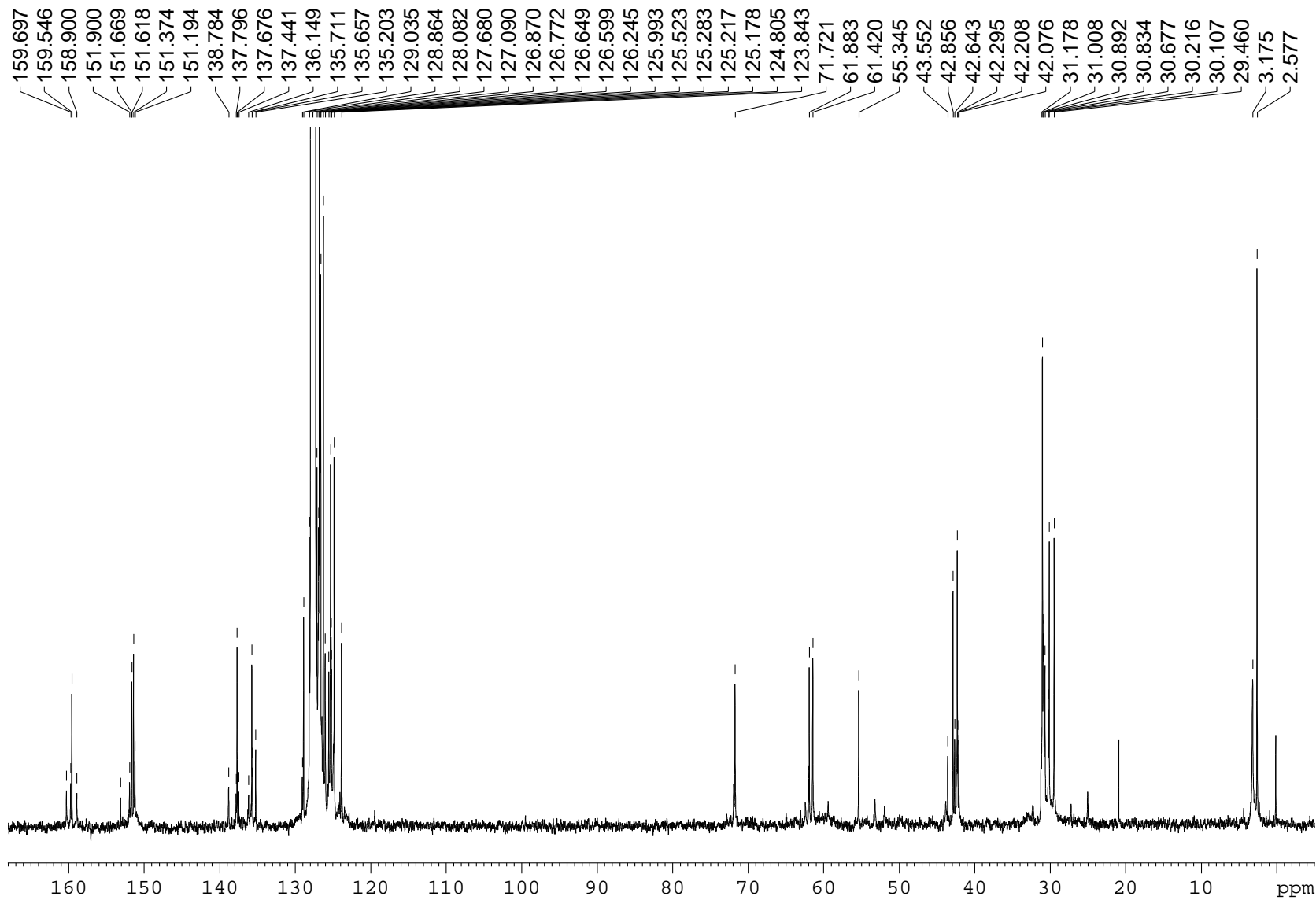
**Figure S20.**  $^{29}\text{Si}\{\text{H}\}$  NMR spectrum (79 MHz,  $\text{C}_6\text{D}_6$ , 298 K) of  $\text{Sc}\{\text{ONOO}^{\text{CumCl}, \text{Me}}\}(\text{N}(\text{SiHMe}_2)_2)$  (**Sc-3**).



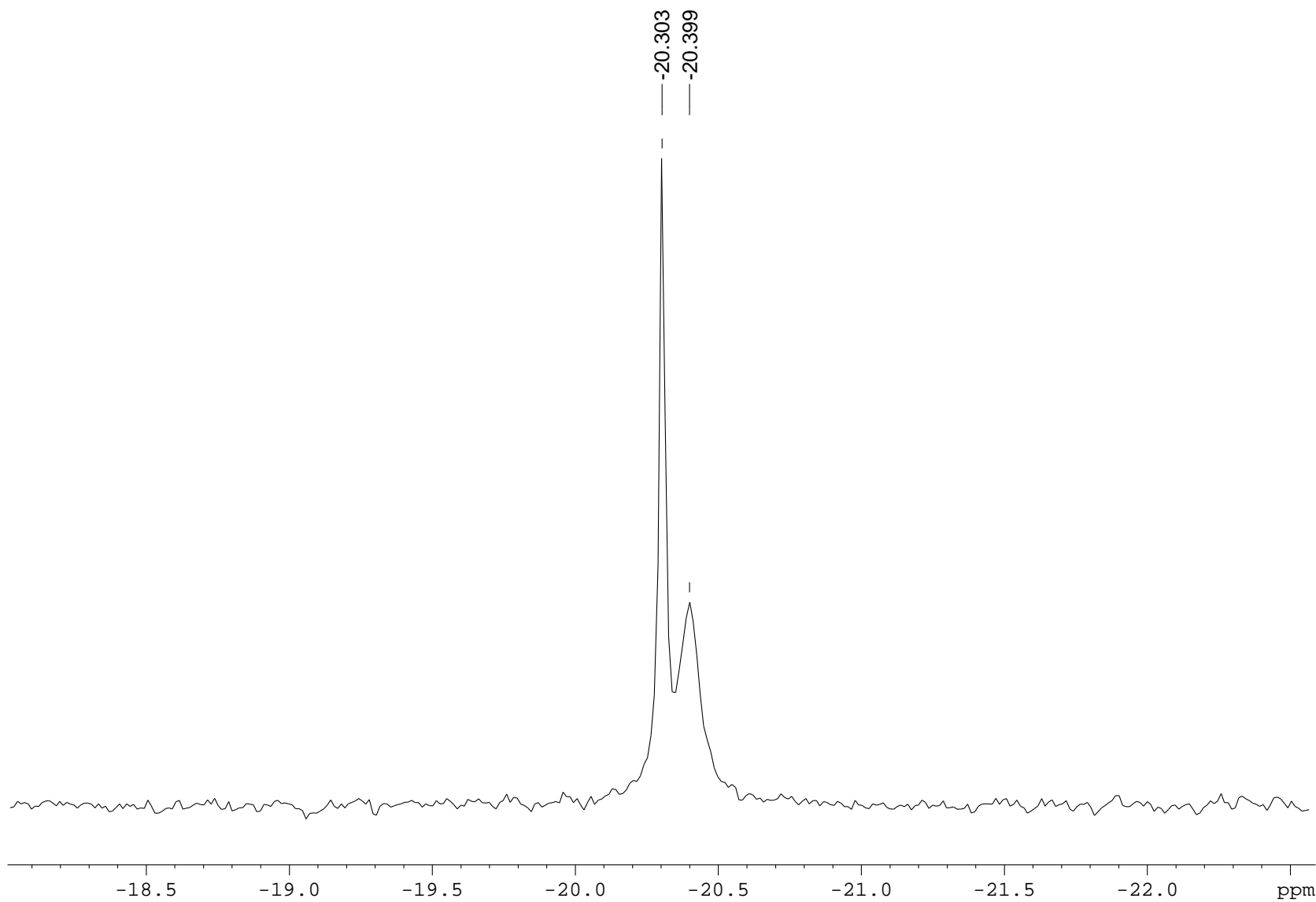
**Figure S21.**  $^{29}\text{Si}$  NMR spectrum (79 MHz,  $\text{C}_6\text{D}_6$ , 298 K) of  $\text{Sc}\{\text{ONOO}^{\text{CumCl},\text{Me}}\}(\text{N}(\text{SiHMe}_2)_2)$  (**Sc-3**).



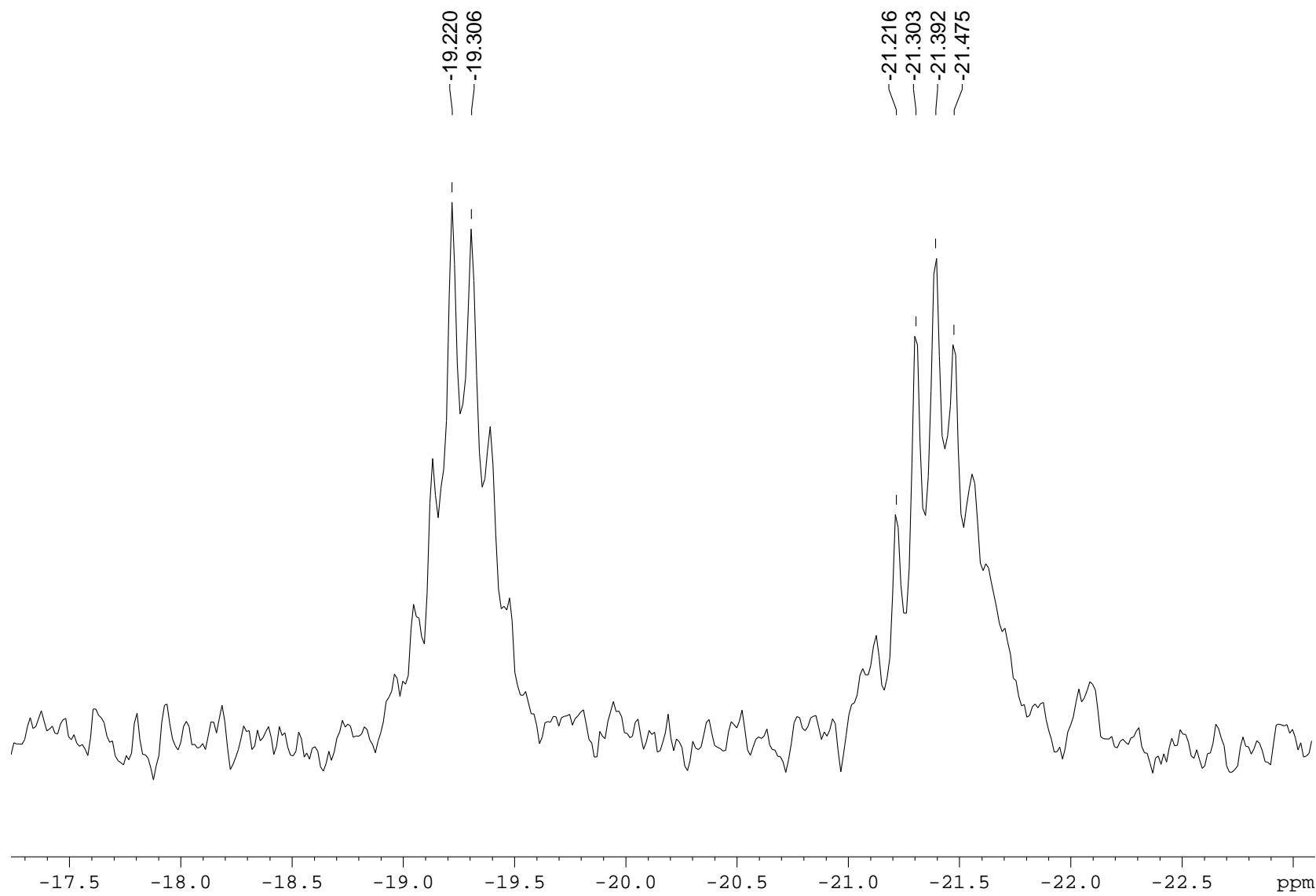
**Figure S22.**  $^1\text{H}$  NMR spectrum (400 MHz,  $\text{C}_6\text{D}_6$ , 333 K) of  $\text{Sc}\{\text{ONOO}^{\text{Cum,Cum}}\}(\text{N}(\text{SiHMe}_2)_2)$  (**Sc-4**).



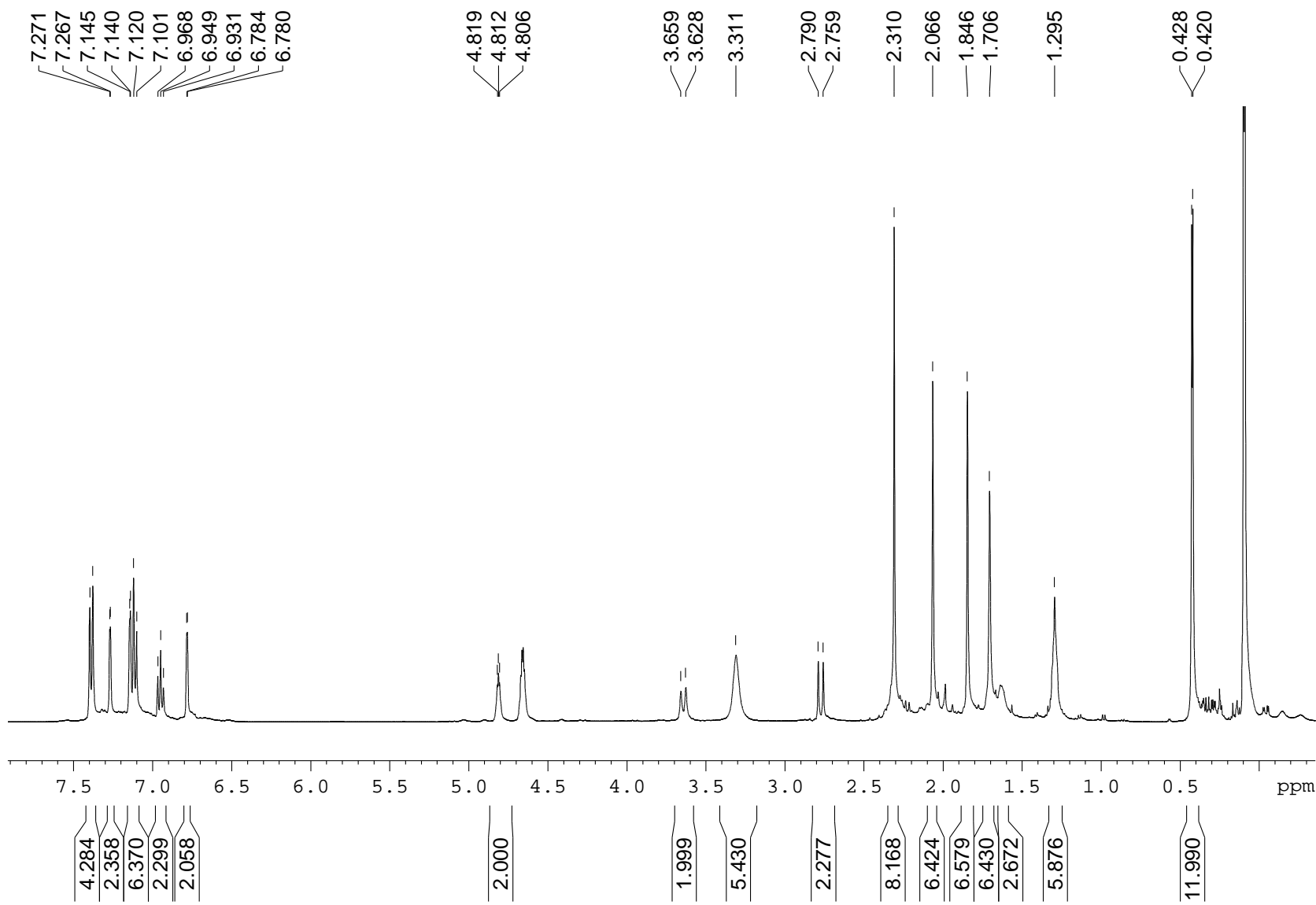
**Figure S23.**  $^{13}\text{C}\{\text{H}\}$  NMR spectrum (100 MHz,  $\text{C}_6\text{D}_6$ , 333 K)  $\text{Sc}\{\text{ONOO}^{\text{Cum,Cum}}\}(\text{N}(\text{SiHMe}_2)_2)$  (**Sc-4**).



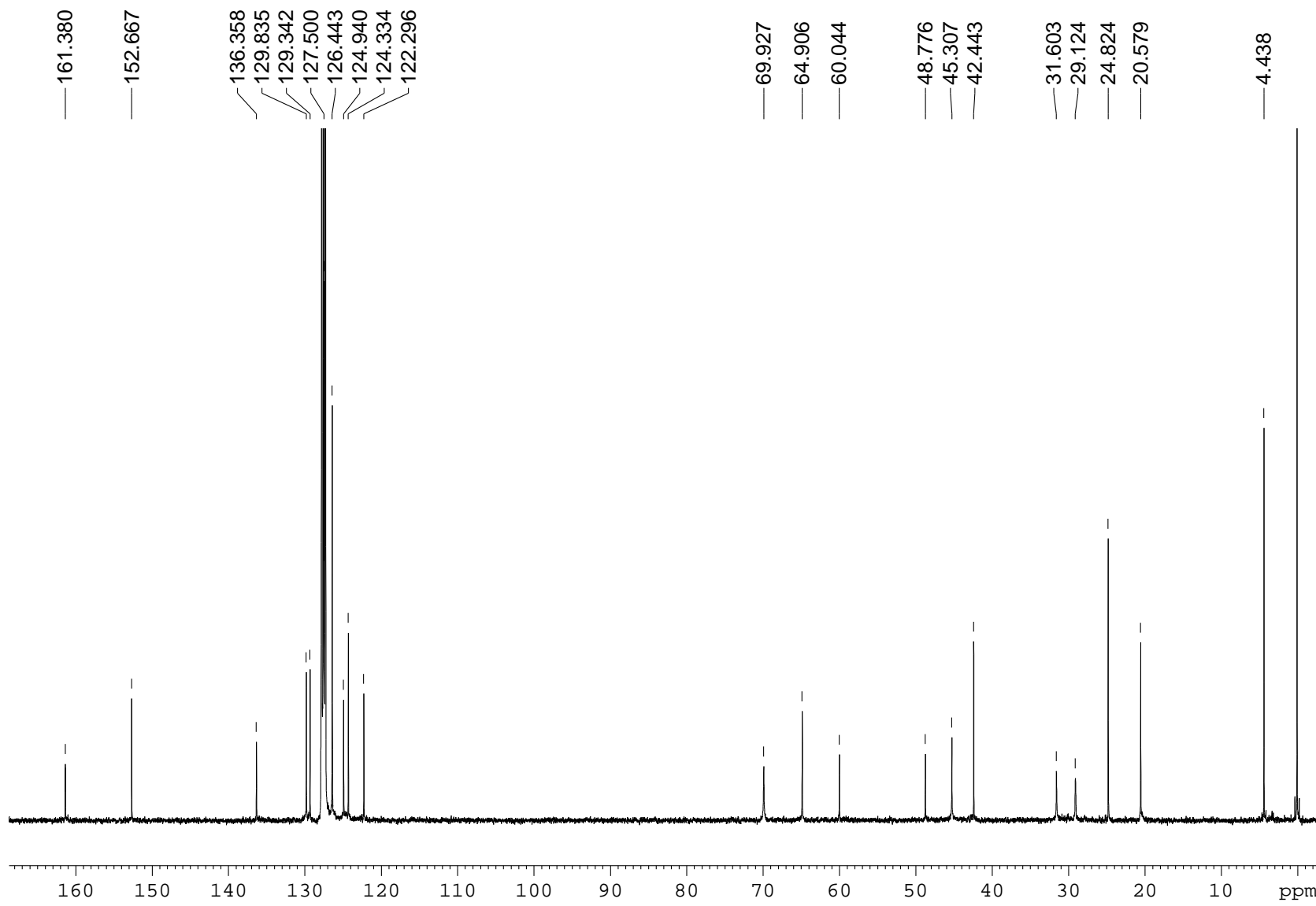
**Figure S24.**  $^{29}\text{Si}\{\text{H}\}$  NMR spectrum (79 MHz,  $\text{C}_6\text{D}_6$ , 333 K) of  $\text{Sc}\{\text{ONOO}^{\text{Cum,Cum}}\}(\text{N}(\text{SiHMe}_2)_2)$  (**Sc-4**).



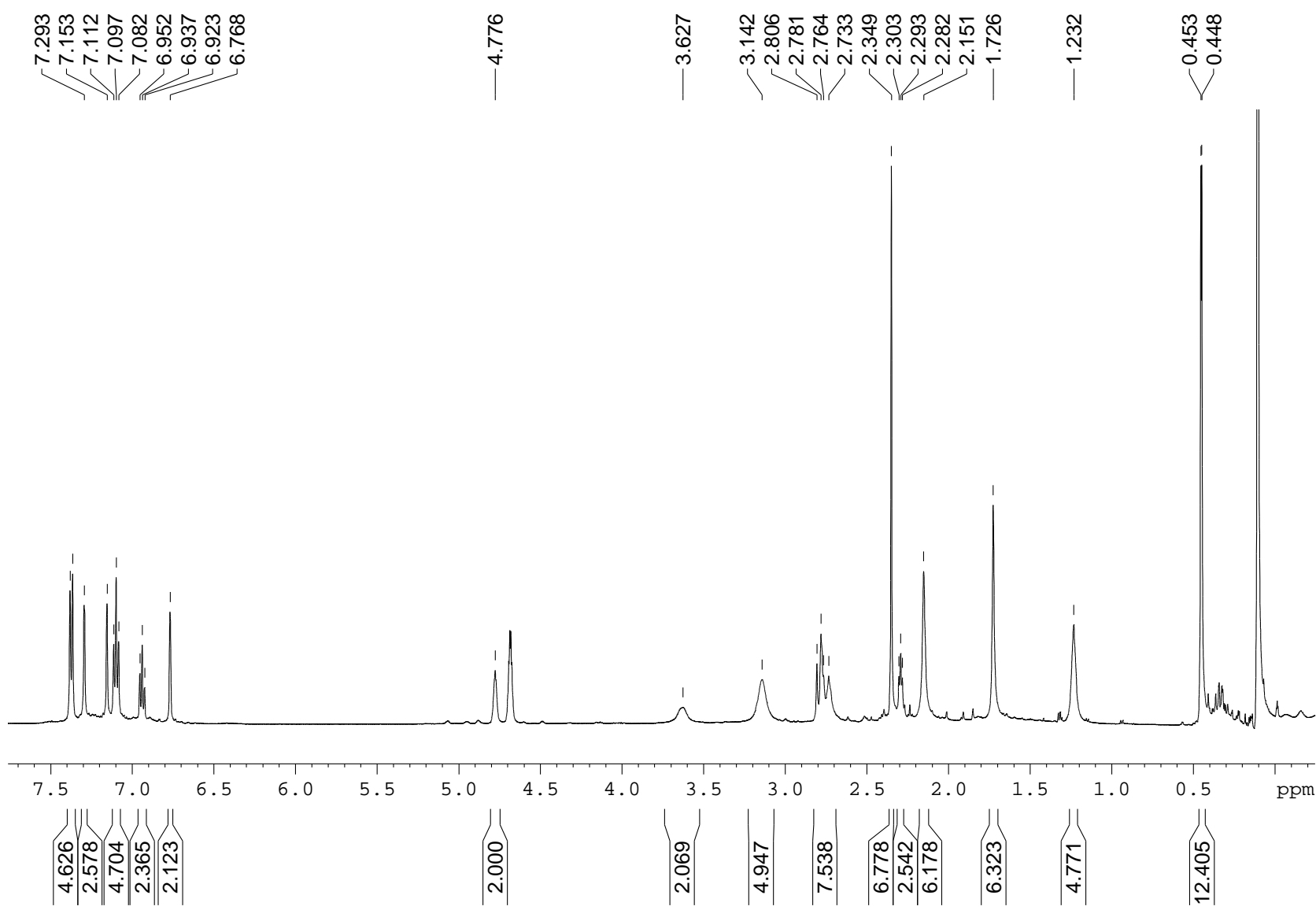
**Figure S25.**  $^{29}\text{Si}$  NMR spectrum (79 MHz,  $\text{C}_6\text{D}_6$ , 333 K) of  $\text{Sc}\{\text{ONOO}^{\text{Cum,Cum}}\}(\text{N}(\text{SiHMe}_2)_2)$  (**Sc-4**).



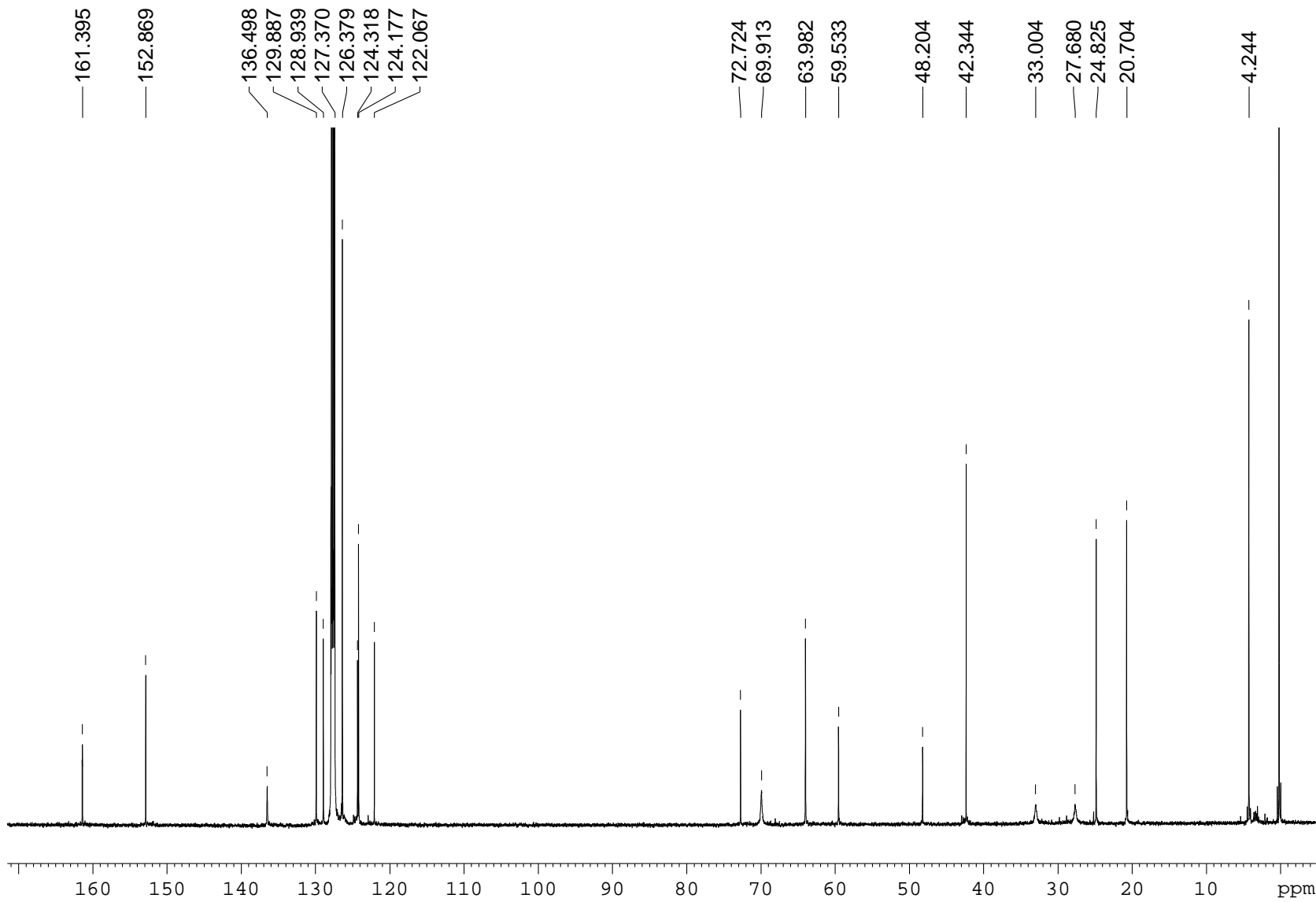
**Figure S26.**  $^1\text{H}$  NMR spectrum (400 MHz,  $\text{C}_6\text{D}_6$ , 313 K) of  $\text{Y}\{\text{ONNO}^{\text{Cum},\text{Me}}\}(\text{N}(\text{SiHMe}_2)_2)\text{THF}$  (**Y-1**).



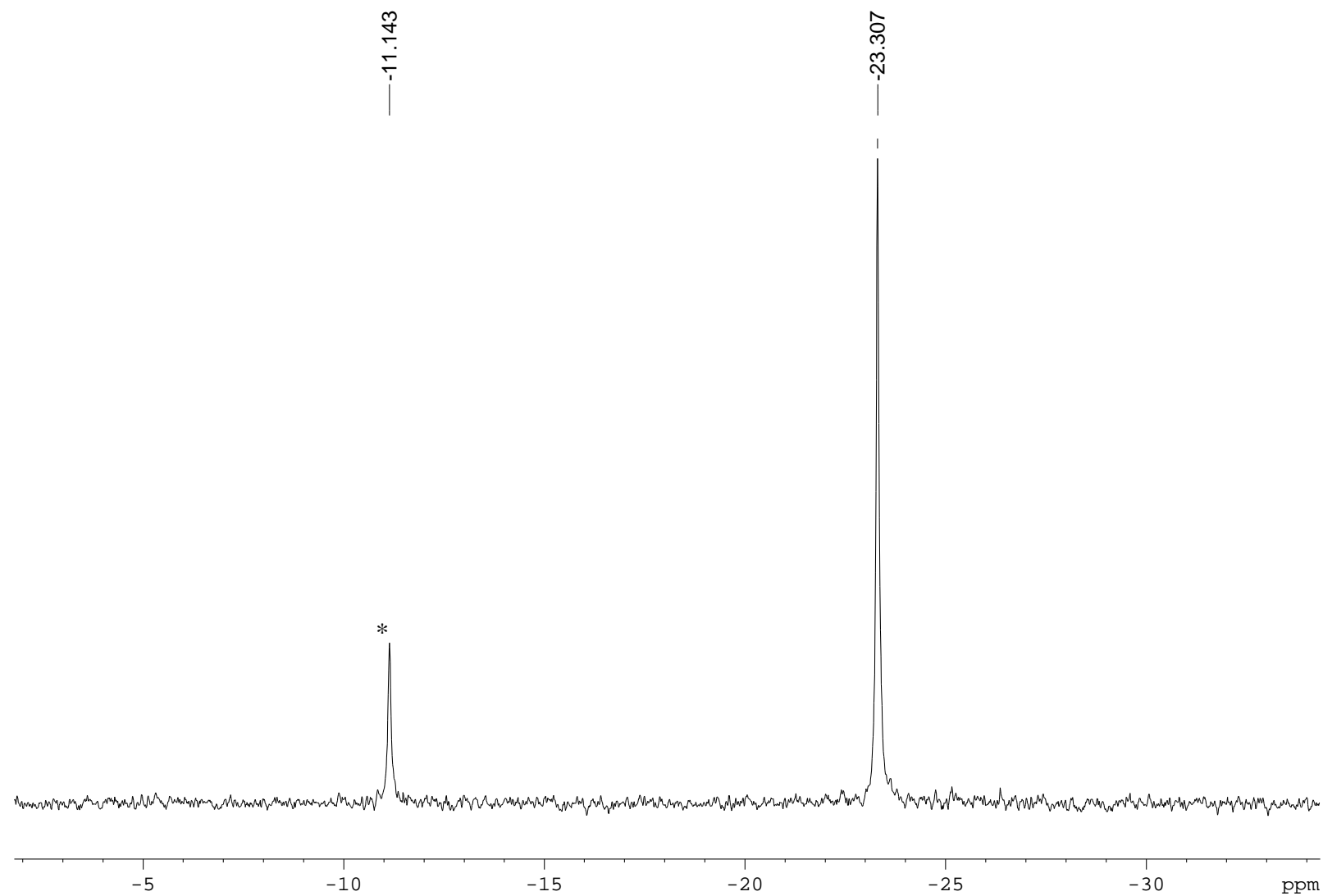
**Figure S27.**  ${}^{13}\text{C}\{{}^1\text{H}\}$  NMR spectrum (100 MHz,  $\text{C}_6\text{D}_6$ , 313 K) of  $\text{Y}\{\text{ONNO}^{\text{Cum},\text{Me}}\}(\text{N}(\text{SiHMe}_2)_2)\text{THF}$  (**Y-1**).



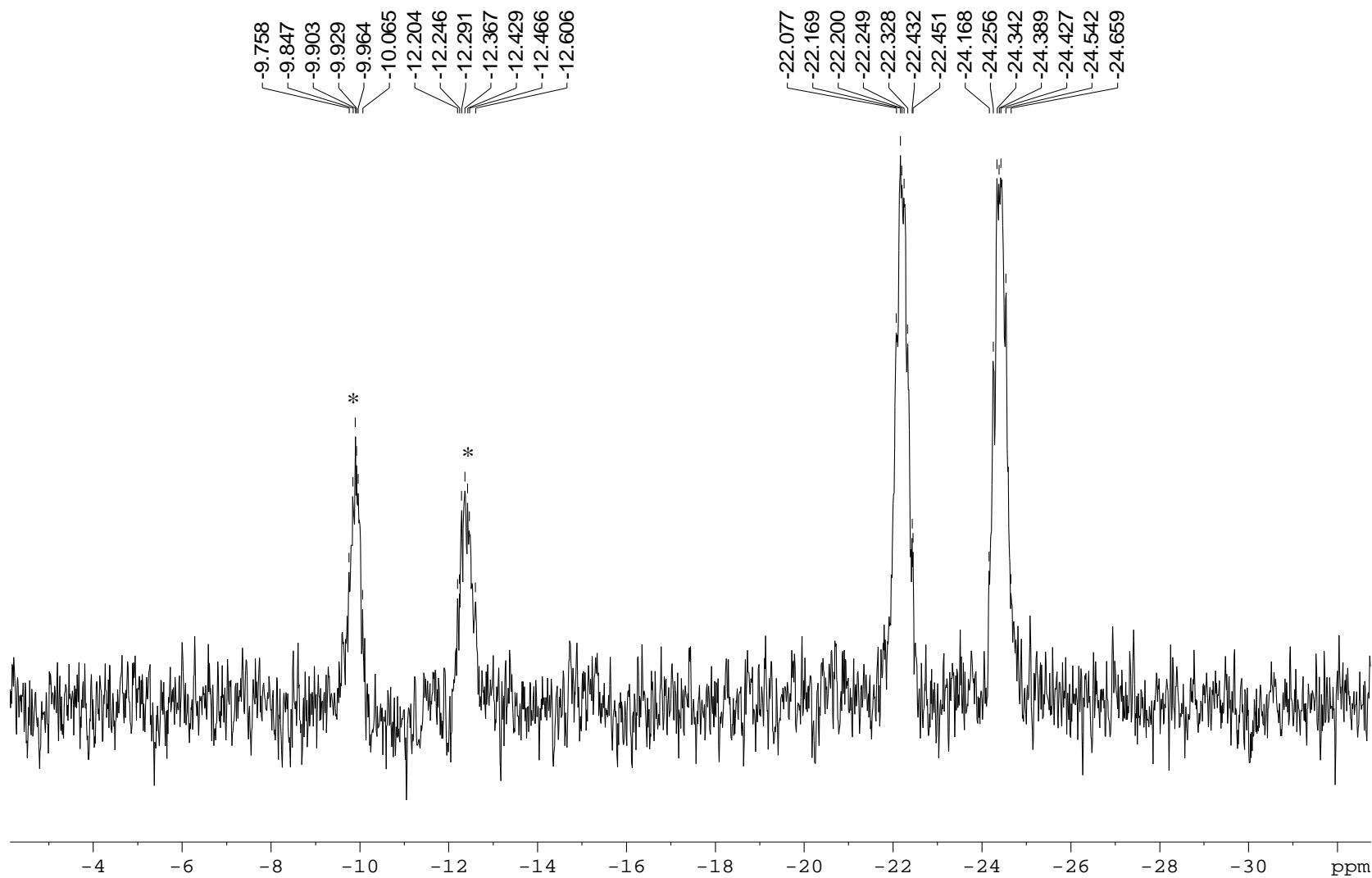
**Figure S28.**  $^1\text{H}$  NMR spectrum (500 MHz,  $\text{C}_6\text{D}_6$ , 298 K) of  $\text{Y}\{\text{ONOO}^{\text{Cum},\text{Me}}\}(\text{N}(\text{SiHMe}_2)_2)\text{THF}$  (**Y-2**).



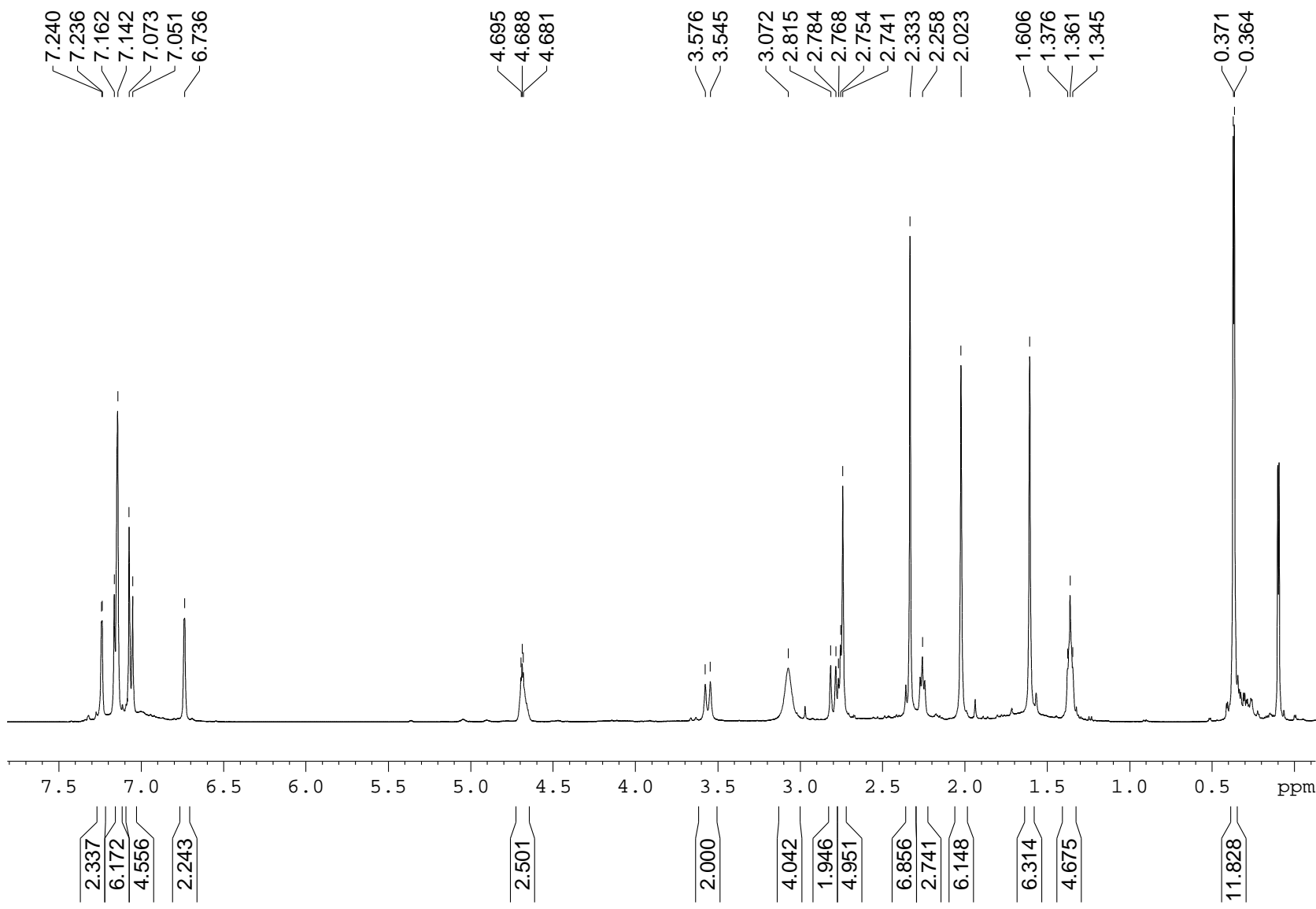
**Figure S29.**  $^{13}\text{C}\{\text{H}\}$  NMR spectrum (125 MHz,  $\text{C}_6\text{D}_6$ , 313 K) of  $\text{Y}\{\text{ONOO}^{\text{Cum},\text{Me}}\}(\text{N}(\text{SiHMe}_2)_2)\text{THF}$  (**Y-2**).



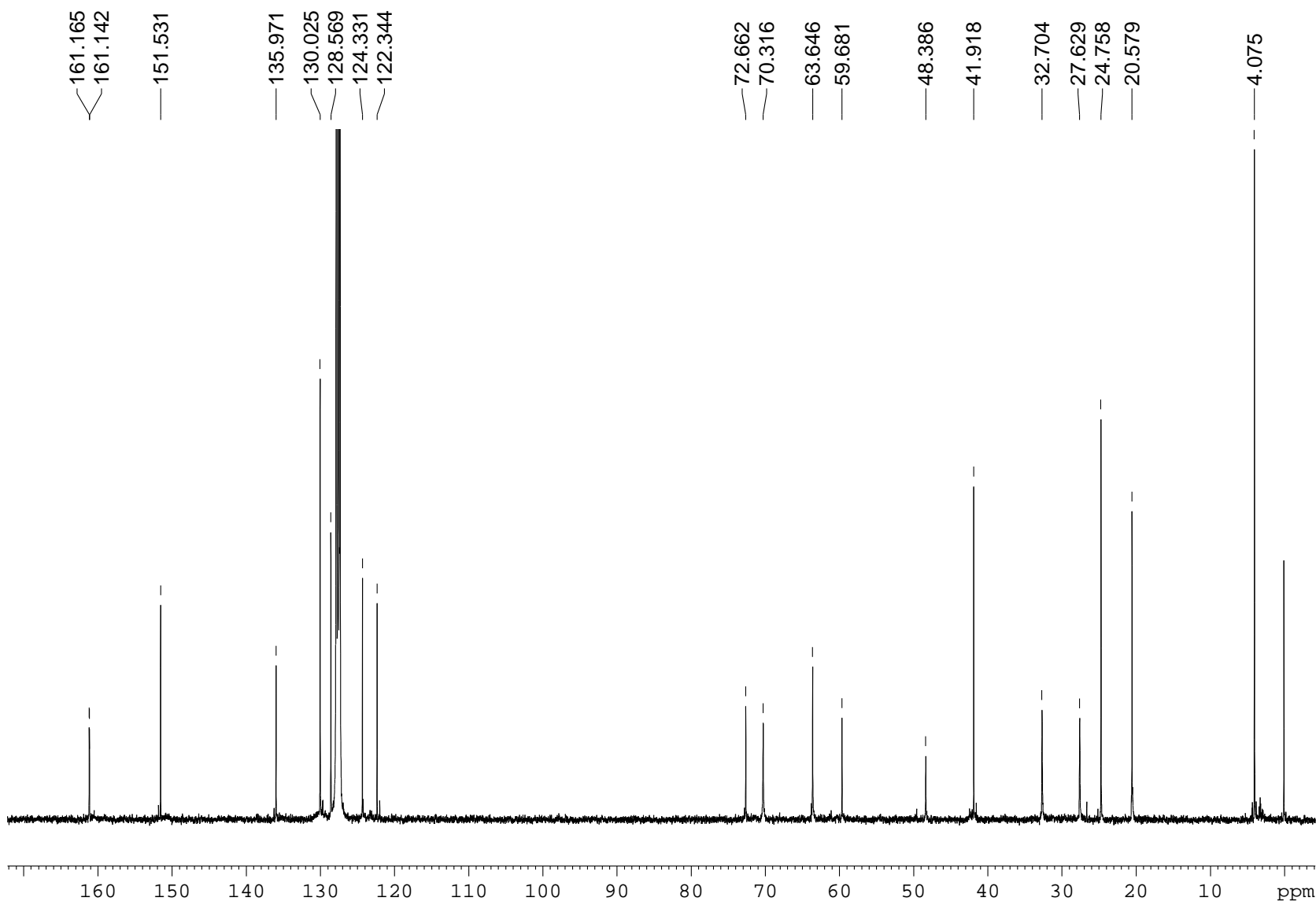
**Figure S30.**  ${}^{29}\text{Si}\{{}^1\text{H}\}$  NMR spectrum (79 MHz,  $\text{C}_6\text{D}_6$ , 313 K) of  $\text{Y}\{\text{ONOO}^{\text{Cum,Me}}\}(\text{N}(\text{SiHMe}_2)_2)\text{THF}$  (**Y-2**). \* stands for residual signal of  $\text{H}_2\text{SiMe}_2$ .



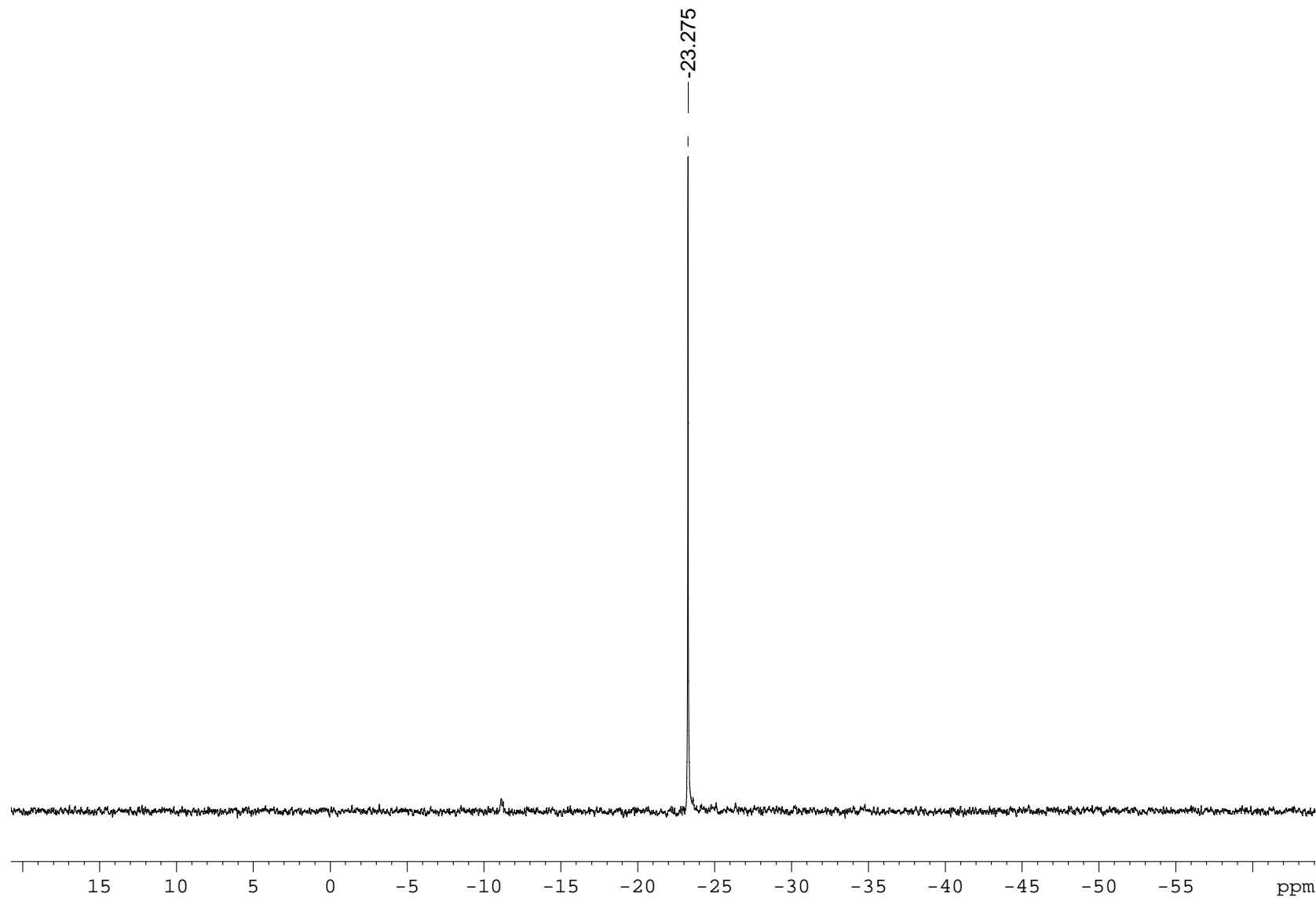
**Figure S31.**  $^{29}\text{Si}$  NMR spectrum (79 MHz,  $\text{C}_6\text{D}_6$ , 313 K) of  $\text{Y}\{\text{ONOO}^{\text{Cum},\text{Me}}\}(\text{N}(\text{SiHMe}_2)_2)\text{THF}$  (**Y-2**). \* stands for residual signal of  $\text{H}_2\text{SiMe}_2$ .



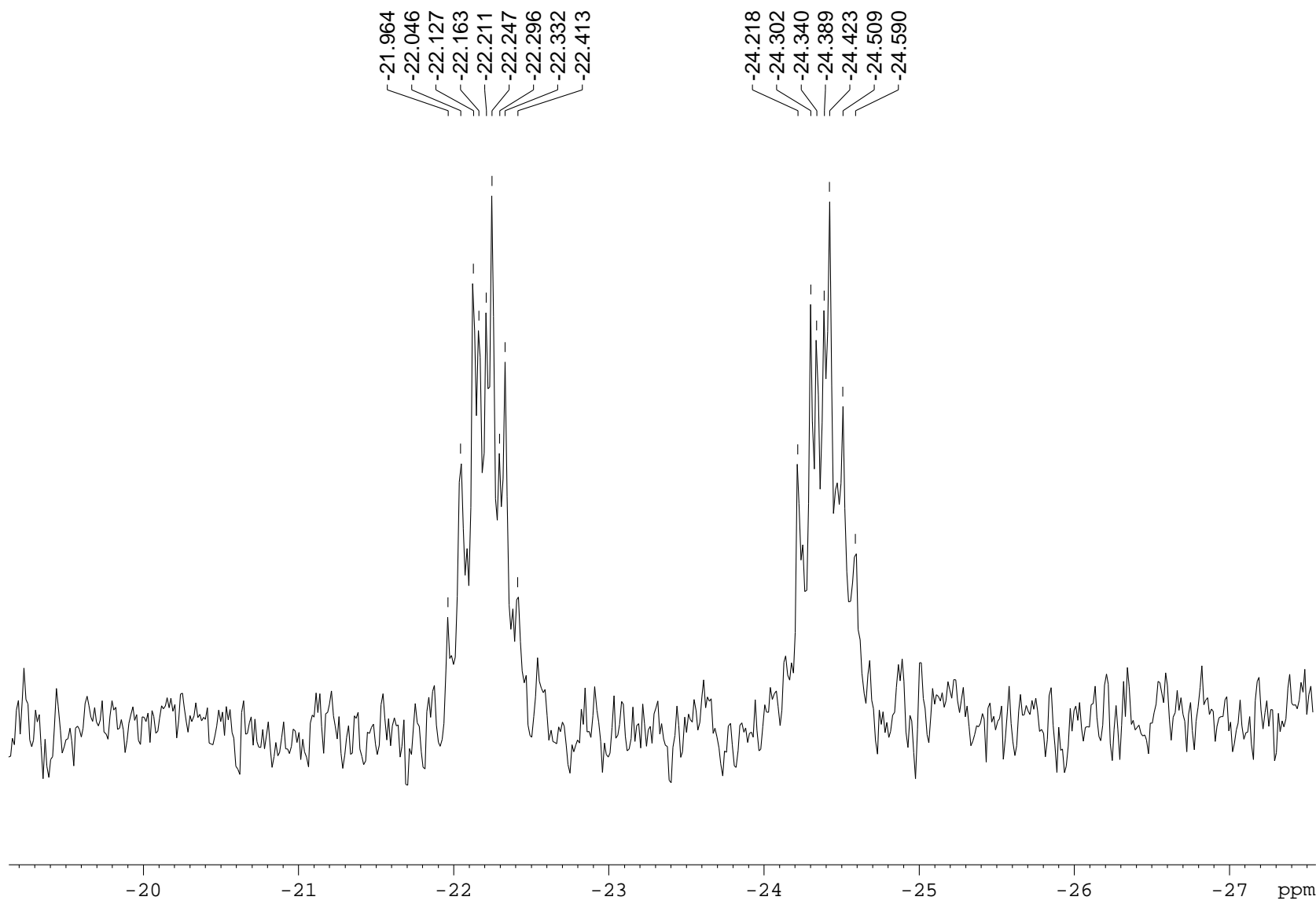
**Figure S32.**  $^1\text{H}$  NMR spectrum (400 MHz,  $\text{C}_6\text{D}_6$ , 333 K) of  $\text{Y}\{\text{ONOO}^{\text{CumCl,Me}}\}(\text{N}(\text{SiHMe}_2)_2)\text{THF}$  (**Y-3**).



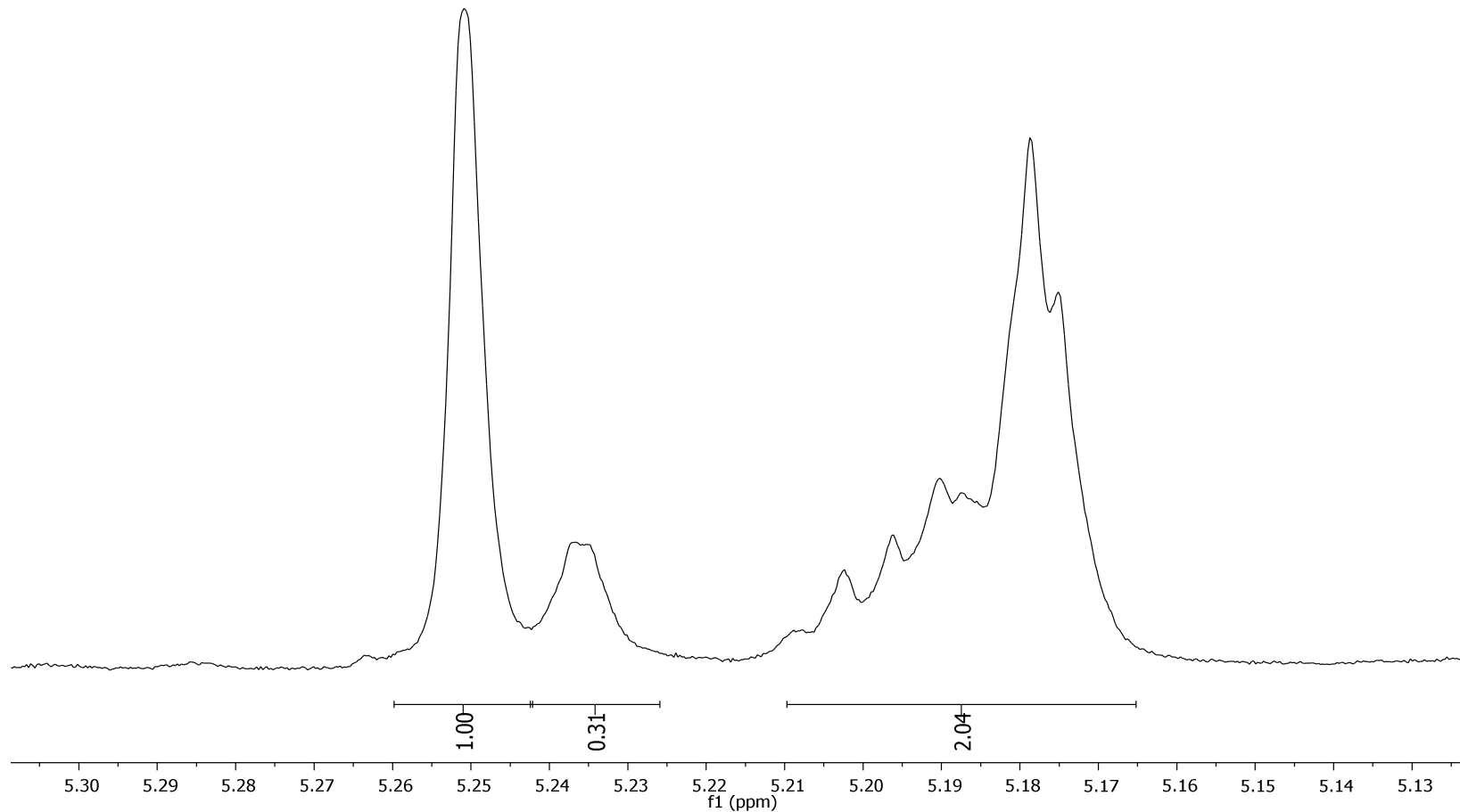
**Figure S33.**  $^{13}\text{C}\{\text{H}\}$  NMR spectrum (100 MHz,  $\text{C}_6\text{D}_6$ , 333 K) of  $\text{Y}\{\text{ONOO}^{\text{CumCl,Me}}\}(\text{N}(\text{SiHMe}_2)_2)\text{THF}$  (**Y-3**).



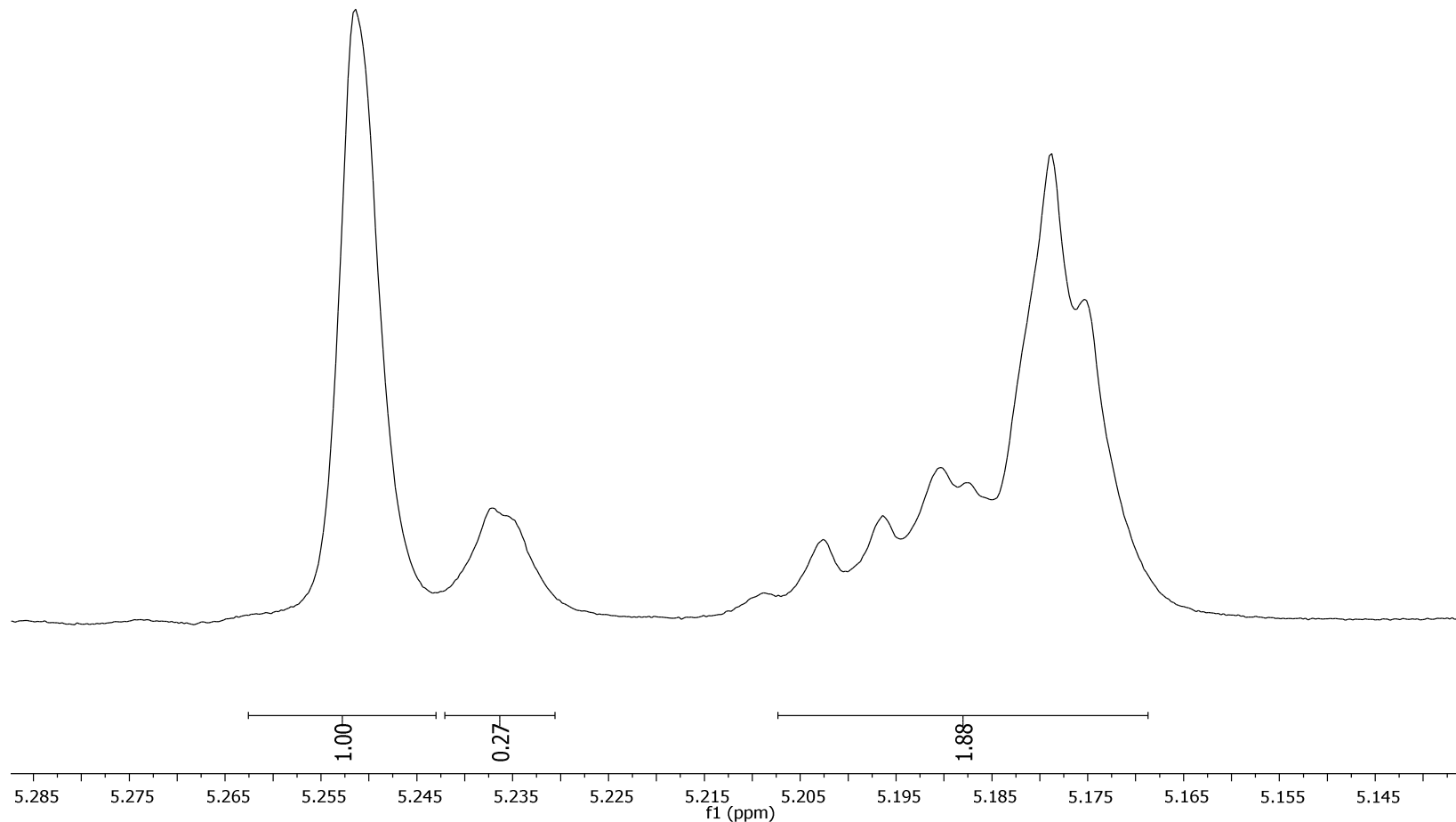
**Figure S34.**  $^{29}\text{Si}\{\text{H}\}$  NMR spectrum (79 MHz,  $\text{C}_6\text{D}_6$ , 333 K) of  $\text{Y}\{\text{ONOOCumClMe}\}(\text{N}(\text{SiHMe}_2)_2)\text{THF}$  (**Y-3**).



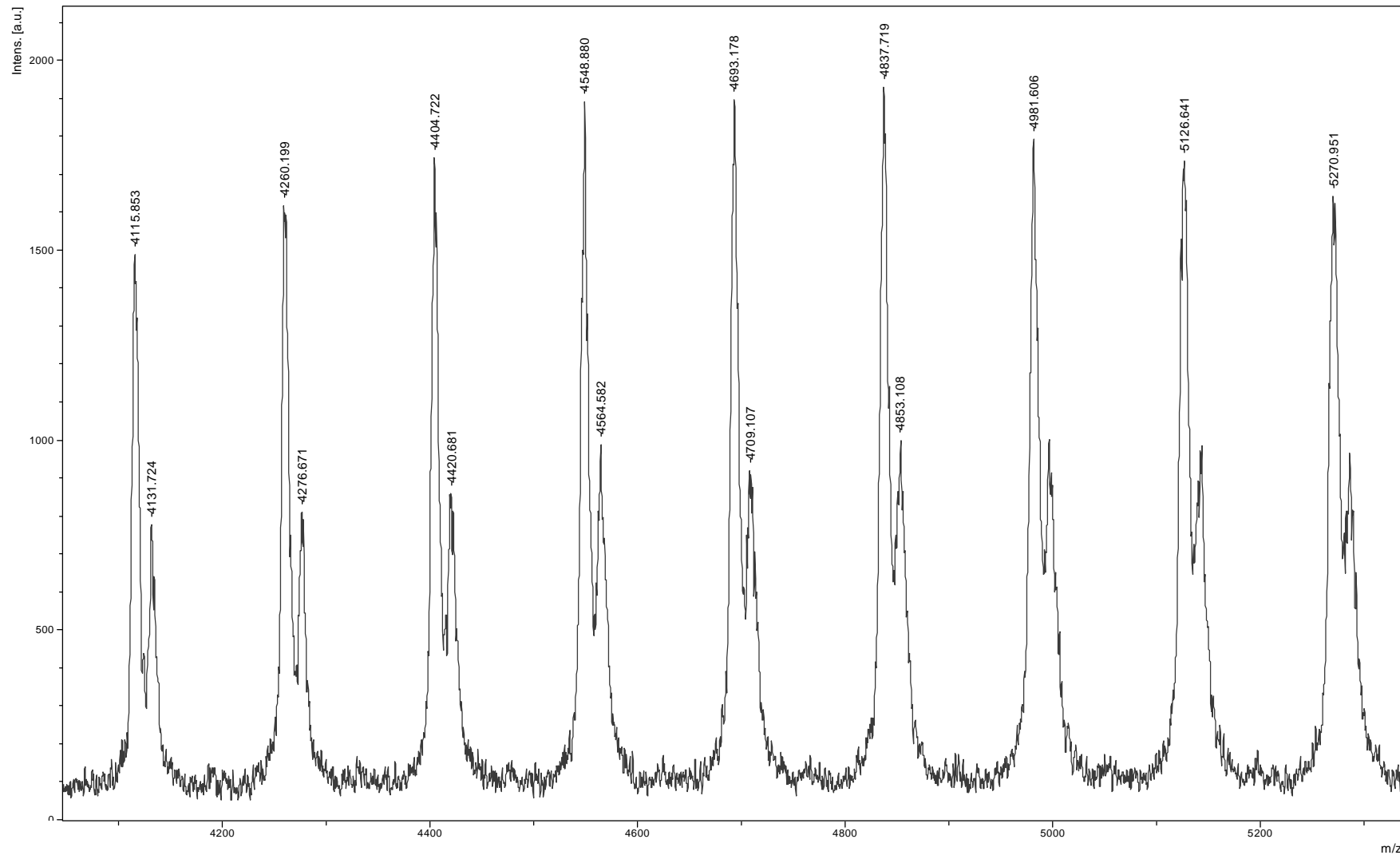
**Figure S35.**  $^{29}\text{Si}$  NMR spectrum (79 MHz,  $\text{C}_6\text{D}_6$ , 333 K) of  $\text{Y}\{\text{ONOO}^{\text{CumCl},\text{Me}}\}(\text{N}(\text{SiHMe}_2)_2)\text{THF}$  (**Y-3**).



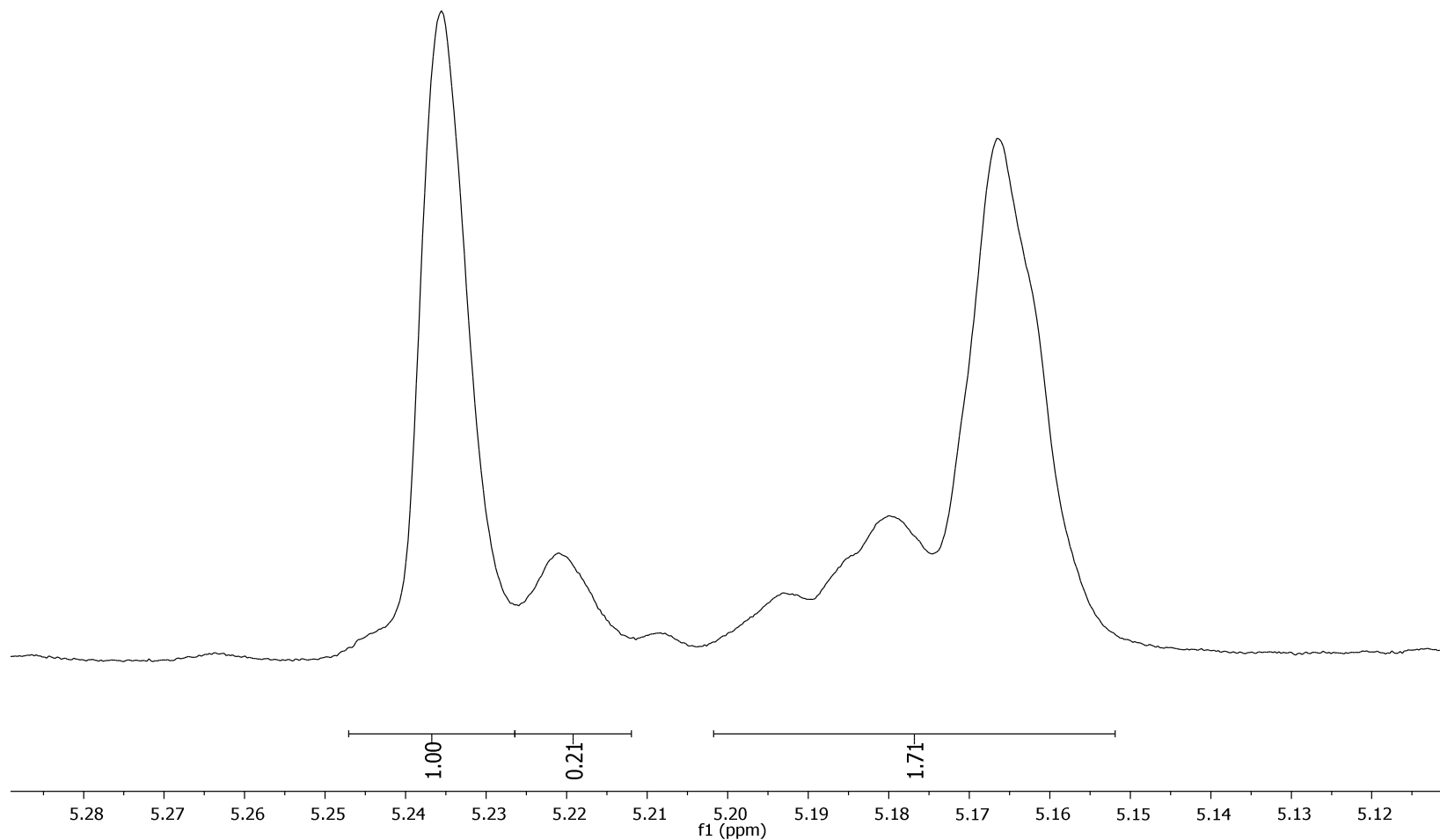
**Figure S36.** Detail of the homo-decoupled methine region of the  $^1\text{H}$  NMR spectrum (500 MHz,  $\text{CDCl}_3$ , 298 K) of a PLA produced from the Sc-**1**/*i*PrOH (1:1) system in toluene ( $P_r = 0.77$ ) (Table 2, entry 3).



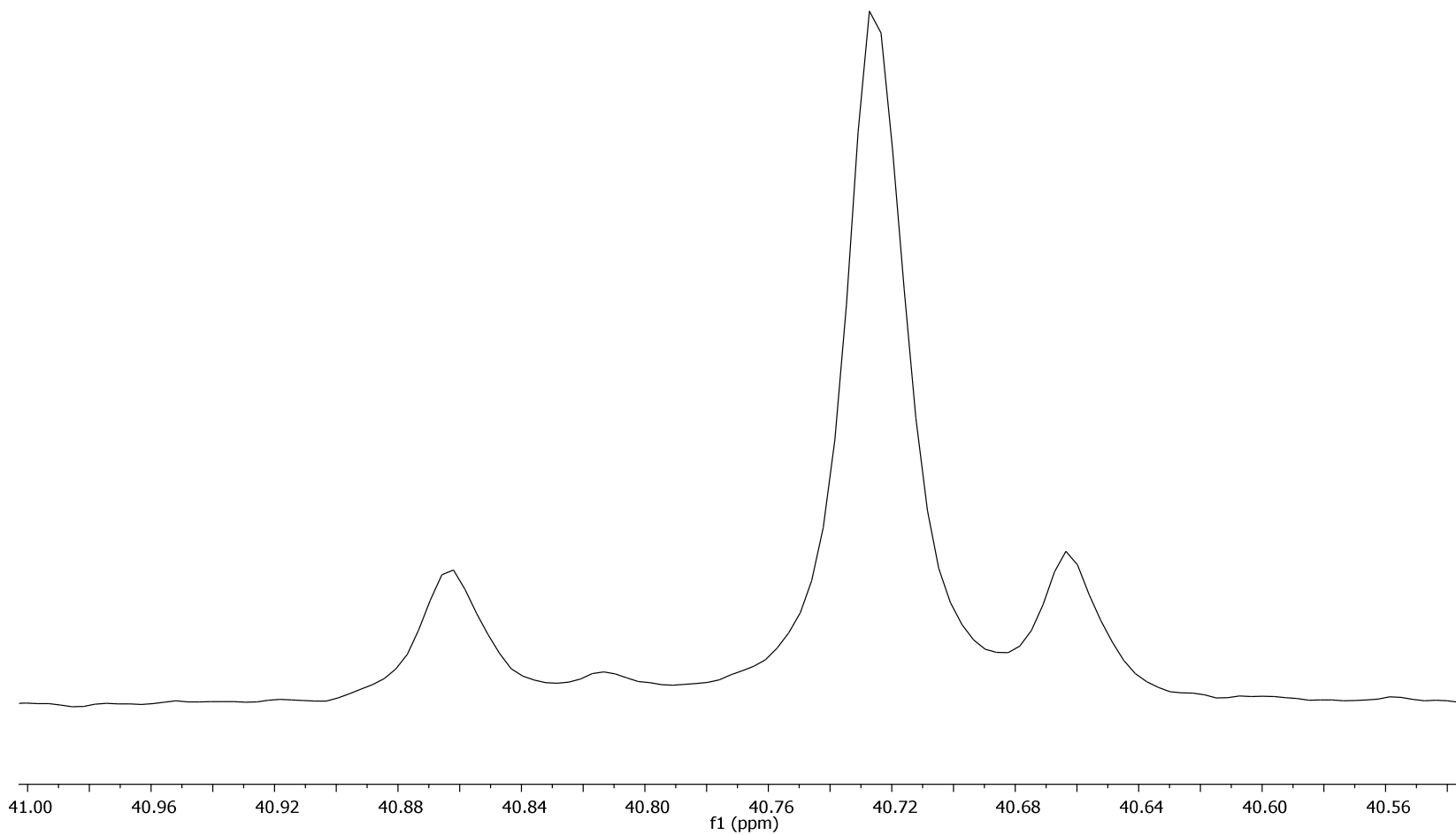
**Figure S37.** Detail of the homo-decoupled methine region of the <sup>1</sup>H NMR spectrum (500 MHz, CDCl<sub>3</sub>, 298 K) of a PLA produced from the Sc-3/iPrOH (1:1) system in toluene ( $P_r = 0.80$ ) (Table 2, entry 10).



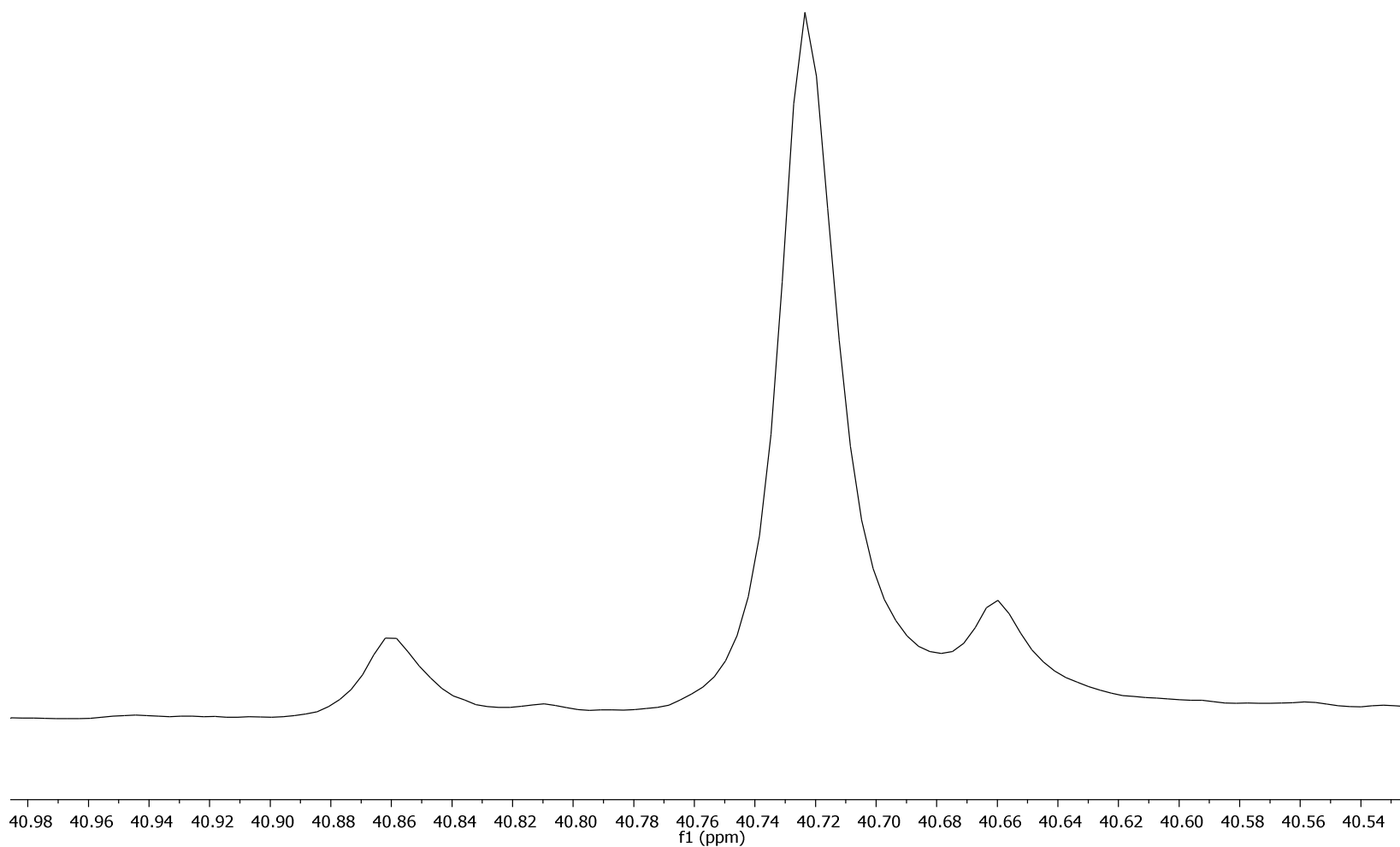
**Figure S38.** MALDI-TOF mass spectrum (main population: Na<sup>+</sup>; minor population: K<sup>+</sup>) of a PLA produced from the Sc-3/iPrOH (1:1) system in toluene ( $P_r = 0.80$ ) (Table 2, entry 12).



**Figure S39.** Detail of the homo-decoupled methine region of the <sup>1</sup>H NMR spectrum (500 MHz, CDCl<sub>3</sub>, 298 K) of a PLA produced from the Sc-4/iPrOH (1:1) system in toluene ( $P_r = 0.83$ ) (Table 2, entry 13).



**Figure S40.** Detail of the methylene region of the  $^{13}\text{C}\{^1\text{H}\}$  NMR spectrum (125 MHz,  $\text{CDCl}_3$ , 298 K) of a PHB produced from the **Y-1** system in toluene ( $P_r = 0.81$ ) (Table 3, entry 6).



**S41.** Detail of the methylene region of the  $^{13}\text{C}\{\text{H}\}$  NMR spectrum (125 MHz,  $\text{CDCl}_3$ , 298 K) of a PHB produced from the **Y-3/iPrOH** (1:1) system in toluene ( $P_r = 0.87$ ) (Table 3, entry 14).